Journal of Rock Mechanics and Geotechnical Engineering 15 (2023) 2757–2777

Contents lists available at ScienceDirect

Journal of Rock Mechanics and Geotechnical Engineering

journal homepage: www.jrmge.cn

Full Length Article

Laboratory investigation on damping characteristics of homogeneous and stratified soil-ash system

Amit Kumar Ram, Supriya Mohanty*

Department of Civil Engineering, Indian Institute of Technology (BHU) Varanasi, Varanasi, 221005, India

ARTICLE INFO

Article history:
Received 27 August 2022
Received in revised form
21 April 2023
Accepted 26 April 2023
Available online 8 July 2023

Keywords:
Homogeneous soil
Stratified soil-ash system
Damping behavior
Cyclic triaxial test
Asymmetric hysteresis loop
Model fitting

ABSTRACT

In this study, the damping responses of uniform soil, equi-proportional fly ash, and local soil as a single unit were investigated. The large-strain cyclic triaxial tests were performed for the specimen compacted at the desired density (95%–99% of maximum dry density). The compacted specimens were tested under the loading frequency of 0.3–1 Hz with medium confinement of 70–100 kPa. Also, the unsymmetrical behavior of the hysteresis loop was analyzed using three different damping estimation approaches, i.e. symmetric hysteresis loop (SHL), asymmetric hysteresis loop (ASHL), and the modified American Society for Testing and Materials (ASTM) method. The outcome of the study shows for fly ash, local soil, and layered soil-ash, the ASHL technique has the highest damping value, followed by ASTM and then the SHL approach. The specimens prepared under high density and subjected to high confinement show low damping values. However, the specimens tested at high frequency exhibits high damping behavior. Similarly, the damping value of fly ash determined using the SHL and ASHL methods has a similar profile and reaches a maximum at 1% shear strain value before decreasing. The composite stratified deposit exhibits more dependency on relative compaction, confining pressure, and less on loading frequency. Based on the results, it is highly recommended to use the ASHL approach, especially under large strain conditions irrespective of soil type. The maximum damping ratio of stratified deposits is always in between the damping ratio of local soil and fly ash. The damping ratio of stratified soil and local soil is slightly larger than that of the other soils, although the damping ratio of fly ash is equivalent to that of the sand and clayey soil. These results may be helpful in the accurate determination of the damping properties of the layered soil-ash system that is required in the seismic response analysis.

1. Introduction

The coal ash produced by thermal power plants is a key source of concern after municipal solid waste. Despite having the second-largest coal production position and fifth-largest coal reserves, India is not able to meet the current power demand from the coal produced. In the year 2020, about 729 million tonnes of coal were produced and 247 million tonnes were imported (Ministry of Coal, 2020). The total electricity produced from the use of coal is attributed to the generation of 2.6 million tonnes of ash per day (CAE, 2021). A thermal power plant with a capacity of 2000 MW will produce roughly 13,200 tonnes of ash per day, with 2200 tonnes of bottom ash and 11,000 tonnes of fly ash (Naresh, 2010). The fly ash generated in 2020–2021 was around 232.56 million tonnes (CAE, 2021) which is projected to be 600 million tonnes by the year 2032 (Tipraj et al., 2019). These generated coal ashes are usually disposed of in the pond near the thermal power plants in slurry form. The slurry of coal ash deposited in a single period of supply is roughly about 2–5 cm thick homogeneous layers (Ishihara et al., 1980). The continuous supply of alternate slurry layers results in the stratification of coal ash deposits that ultimately leads to the formation of a heap of several meters. Due to the high moisture content, the created heaps are prone to liquefaction and collapse after an earthquake. In the recent decade (2010–2020), 76 coal ash pond accidents occurred as a result of ash dike failure and pipe bursting delivering ash slurry (Shah and Narayan, 2020). The ash pond failures significantly affect the surface water bodies, agricultural lands, property, health of humans and animals, etc.

* Corresponding author.
E-mail address: supriya.civ@iitbhu.ac.in (S. Mohanty).
Peer review under responsibility of Institute of Rock and Soil Mechanics, Chinese Academy of Sciences.

https://doi.org/10.1016/j.jrmge.2023.04.016

Table 1
Summary of the past literature associated with stratified/layered deposit.

Source	Soil type	Preparation method	Parameters		Key findings
			f (Hz)	σ_c' (kPa)	
Ishihara et al. (1980)	Tailing materials	Pluvial spreading through air; Pluvial spreading through air with tapping; Pluvial spreading through air with vibratory compaction	1	50 or 100	Non-plastic fine tailing shows lower strength than that of plastic tailing having PI of 15–20
Fiegel and Kutter (1994)	Layered silt and sand	Dry pluviation through air (centrifuge model tests)	1		The development of pore pressure in layered soil deposits differs from the generation of pore pressure in uniform soil deposits
Amini and Sama (1999)	Stratified sand-silt-gravel	Moist tamping (homogeneous); Sedimentation (stratified)		100	For both uniform and stratified soil conditions, increasing the silt content increases the liquefaction resistance of sand-silt-gravel combinations
Amini and Qi (2000)	Stratified silty sands	Moist tamping; Wet pluviation		50–250	The sample prepared for uniform and stratified soil shows dissimilar soil fabric but that results in not significant variation in liquefaction resistance
Konrad and Dubeau (2003)	Stratified sand-silt	Pluviation under water	0.2	100	Layering caused a substantially lower cycle resistance than either of the materials in undrained cyclic triaxial testing on stratified sand-silt samples
Amini and Chakravrty (2004)	Layered sand-gravel	Pluviation through air (homogeneous); Wet pluviation (layered soil)		50–250	For both homogeneous and layered sand-gravel composite, the liquefaction resistance decreases with increase in confining pressure
Yoshimine and Koike (2005)	Stratification of clean due to segregation	Air pluviation method	0.1	100	Under the same modified relative density, the uniformly deposited material expresses lower resistance to liquefaction than that of stratified one
Jia and Wang (2013)	Stratified sand with silt content	Water sedimentation method	1	100	The liquefaction resistances of layered sands are significantly influenced by the thickness of the silt seam sandwiched in the sand samples
Ayoubi and Pak (2017)	Nevada sand	Air pluviation method	1–10	96	The settlement induced due to liquefaction increases with the width of the footing
Jin et al. (2018)	Tailing materials	Slurry method	2		The tailings dam failure lacks a clearly visible slip surface, but the failure mode reveals overall sliding
Xiu et al. (2020)	Fine and powdery sandy particles	Soil sedimentation	1	50	The thickness of the powdery interlayer has a nonlinear relationship with the cyclic loading necessary for liquefaction

Note: f - frequency, σ_c' - effective confining pressure.

In the present scenario, the major challenging task for geotechnical engineers is to recommend various techniques for the bulk utilization of coal ash. This will be feasible only after knowing the basic/fundamental properties and the response of coal ash under static and dynamic loading conditions. Many of the past studies covered the evaluation of the engineering properties of coal ashes. However, sustainable and better performance of the structures resting on coal ash requires thorough investigation prior to its field applications. Therefore, it is significant to perform ground response analysis that will render the site's natural periods, ground motion amplification, response spectra, liquefaction potential, and seismic stability of slopes (Govindaraju et al., 2004). Since the disposal of coal ash forms a stratified/layered structure, hence its response must be evaluated thoroughly. The factors on which the ground response analysis depends are motion frequency (base), the geometry of the deposit, properties of the material, etc. (Sitharam and Anbazhagan, 2008). For the safe design of geotechnical structures on stratified deposits under seismic conditions, the response spectrum of several layers should be determined (Kumar and Dey, 2015). In order to accomplish ground response analysis, it is necessary to evaluate its dynamic properties. The dynamic properties such as maximum shear modulus (G_{max}), dynamic shear modulus (G), and damping ratio (D) used for the response analysis must be presented in the form of a modulus reduction curve (G/G_{max} versus γ) and damping ratio curve (D versus γ) (Chen et al., 2007; Kumar et al., 2017; Puri et al., 2020).

Past studies mostly examined the dynamic properties of reconstituted homogeneous samples and two mixed coal ash materials (Jakka et al., 2010; Liao et al., 2012; Yoshimoto et al., 2014; Mohanty and Patra, 2016; Chattaraj and Sengupta, 2017; Reddy et al., 2020). Layered/stratified soil structures generally exist in the form of tailings dams, alluvial and hydraulic fill deposits, the foundation of buildings, sedimentary strata, lacustrine, marine deposits, and pavement subgrade layers (Amini and Chakravrty, 2004; Xiu et al., 2020). The use of dynamic properties evaluated from the homogeneous soil for stratified deposits may lead to erroneous results (or may overestimate/underestimate). The dynamic failure mechanism of the stratified deposit is significantly different from that of a homogeneous deposit, which has been properly explained by Fiegel and Kutter (1994) by employing the centrifuge model test. It has been observed from the model test that an apparent water gap was generated between two layered soils during liquefaction. Due to the increase in pore pressure, the apparent water at the interface develops the tendency to counterbalance the overburden pressure. This results in zero effective stress condition that ultimately fails the overlying layer and high-velocity flow occurs. Various studies focus on the liquefaction characteristics of sand-silt-gravel composite, stratified silty sands, Ottawa sand-silica silt, sand-gravel composite, segregated sand particle's stratification, stratification of coarse and fine sand, etc. (Amini and Sama, 1999; Amini and Qi, 2000; Konrad and Dubeau, 2003; Amini and Chakravrty, 2004; Yoshimine and Koike, 2005; Jia and Wang, 2013; Ayoubi and Pak, 2017; Jin et al., 2018; Xiu et al., 2020). Also, a summary of past literature on the dynamic studies of stratified soil deposits is listed in Table 1.

The damping ratio exhibits a greater degree of change than the dynamic shear modulus, particularly under high strain. Therefore, it is important to ascertain the damping behavior of soil that has been subjected to a load that produces high strain. Bender element test, resonant column test, and cyclic triaxial test are normally used under very small ($<10^{-6}$), small to medium (10^{-6} to 10^{-3}), and high strain ($>10^{-3}$) conditions, respectively (Ingale et al., 2017). Kalinski and Wallace (2011) observed a high damping value for fly ash compared to typical soils due to its soft nature and determined the shear wave velocity in the range of 110–150 m/s for fly ash. However, Saride and Dutta (2016) stabilized the expansive soil with fly ash and found a decrement in damping behavior with the increment of fly ash. The higher damping was generally due to the rearrangements of particles and a high tendency of particle slippage (Fahoum et al., 1996). Chattaraj and Sengupta (2017) considered both the resonant column and cyclic triaxial tests to determine the damping ratio of fly ash and sand. Regardless of the confining pressure, it was discovered that the damping ratio of sand is always greater than that of fly ash. Most of the studies were primarily focused on the damping characteristics of sand. Hardin (1965) stated that loading frequency has a significantly lower impact on the damping characteristics as compared to other parameters. According to Kokusho (1980), soil damping is more likely to be hysteretic than viscous. Similarly, Borden et al. (1996) observed an increasing trend of damping value with the increment in the shear strain at a faster rate for clay and a slower rate for sand. Also, the influence of shear strain is more promising than the confining pressure on damping magnitude. Santos and Correia (2000) demarcated the damping versus shear strain plot into two parts (linear threshold and volumetric threshold shear strain) to identify the initiation of nonlinear behavior. The linear elastic range is supposed to have zero energy dissipation (Zhang et al., 2005). Paul and Dey (2007) found that the damping ratio is inversely proportional to the effective confining pressure. This inverse relationship exists due to the increase in stiffness of the specimen with the increase in effective confining pressure (Kumar et al., 2017). The damping versus shear strain plot will shift down-rightward with the gradual increase of confining pressure (Dammala et al., 2017).

The damping ratio is commonly estimated using a symmetric hysteresis loop (SHL) formed in the shear stress versus shear strain plot. In the cyclic triaxial test, the SHL gets converted into an asymmetric hysteresis loop (ASHL), especially under large shear strain observed in various studies (Kokusho, 1980; Jaya et al., 2012; Kumar et al., 2017). A "spindle-shaped" hysteresis loop was observed at a small strain, whereas an "S-shaped" hysteresis loop was observed under a large strain, according to Nogami et al. (2012). Kumar et al. (2017) incorporated the ASHL for the damping evaluation and found a unique profile of the damping versus shear strain, which increases with shear strain and attains a maximum at 1% shear strain and then decreases continuously. On the other hand, most of the past studies considered only symmetric loop and showed the continuously increasing profile of the damping versus shear strain. Chakrabortty et al. (2020) and Das and Chakrabortty (2021) considered ASHL and modified the ASTM method along with the conventional method to determine the variation in damping ratio. From the results, it was concluded that symmetric methods underestimate the damping value, whereas asymmetric method gives a higher damping value. Mog and Anbazhagan (2022) also implemented two approaches (steady state vibration (SSV) and free vibration decay (FVD)) in the resonant column test. It is advised to use the SSV approach for small strains, whereas the FVD method may work better for medium strains.

From the above-mentioned literature, this can be concluded that most of the research is focused on the liquefaction study of stratified sandy materials. Apart from that, past studies are associated with a limited number of variables (e.g. single loading frequency) which can be seen in Table 1. In addition, these samples are subjected to very narrow shear strain during cyclic loading. Furthermore, the dynamic characteristics, particularly the damping behavior of stratified soil deposit is different from that of the homogeneous soil deposit, and very limited studies have been carried out considering the stratification of waste materials and their damping properties. Therefore, it is significant to investigate the damping characteristics of the stratified soil (soil-ash) deposit for the safe design of geotechnical structures resting on it. Also, the

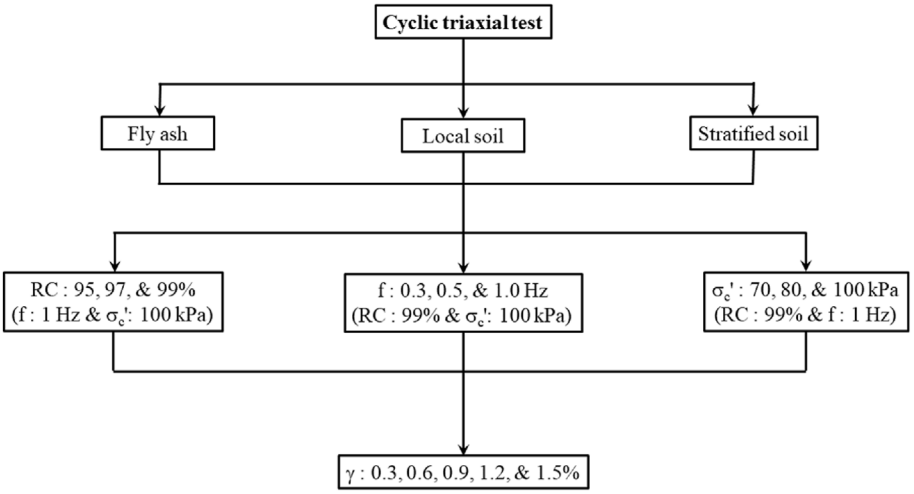

Fig. 1. Schematic experimental plan of testing program.

specimen preparation techniques used in the past studies were cumbersome and time-consuming, which can be eliminated by employing the simple technique used in the present study.

The research gap discussed above from the literature gives the motivation for the present investigation, which has been fulfilled by performing experimental determination of the damping characteristics of uniform and stratified soil-ash deposits using cyclic triaxial tests. The influences of relative compaction, loading frequency, and confining pressure on the damping ratio with varying shear strain have been implemented for a better understanding of the composite system. In addition, the influence of the shape of the hysteresis loop on the damping characteristics has been evaluated using three different methods including SHL, ASHL, and the modified American Society for Testing and Materials (ASTM) method. The precise estimation of the damping ratio helps in the close prediction of ground responses under seismic excitations.

The significance of the present study must be emphasized so that it can be better correlated with the field investigation which will increase its widespread acceptability during the application. As a result, this section explains the necessity of the present study in the current context. The quantity of coal ash produced every year creates a huge amount of accumulation near the ash disposal location. These disposal locations are not properly designed to sustain such huge loads that give rise to the failure of such dams due to the deposition of consecutive layers every year. In order to minimize the disastrous effect of coal ash on the environment, a new practical application area/material must be proposed. The present study specifically concentrated on the application of fly ash as pavement subgrade or embankment fill material. The pavement construction involves a considerable amount of capital, therefore a complete study is required under static and dynamic loading conditions before the application of fly ash in the field. Hence, an attempt has been made here to determine the damping properties of homogeneous and layered soil-ash deposits. Because the damping properties of the material have a substantial impact on the behavior of the deposit under seismic conditions.

The present work examines the damping characteristics of fly ash and local soil in the form of uniform and stratified arrangements. A total of 105 strain-controlled cyclic triaxial tests were performed in the present study. A detailed schematic experimental plan/testing program is shown in Fig. 1. The input variables like relative compaction, frequency of loading, confining pressure, and cyclic shear strain have been considered for the study. Both the uniform and stratified soil-ash samples (50 mm in diameter and 100 mm in height) were prepared under relative compaction (RC) of 95%, 97% and 99%. The tests were conducted under the cyclic shear strain (γ) of 0.3%–1.5% considering loading frequencies of 0.3 Hz, 0.5 Hz and 1 Hz. The confining pressures of 70 kPa, 80 kPa and 100 kPa have been taken into consideration to examine the

Table 2
Fundamental properties of fly ash and local soil.

Geotechnical property	Value	
	Fly ash	Local soil
Content of sand (%)	61.52	2.12
Content of silt (%)	33.19	81.77
Content of clay (%)	5.29	16.11
D_{10} (mm)	0.004	0.0009
D_{30} (mm)	0.018	0.0034
D_{60} (mm)	0.088	0.01
C_u	22	10.53
C_c	0.92	1.22
G	2.35	2.52
MDD (g/cm^3)	1.26	1.73
OMC (%)	30.5	16.4
Classification	Silty sand	Silt of intermediate plasticity

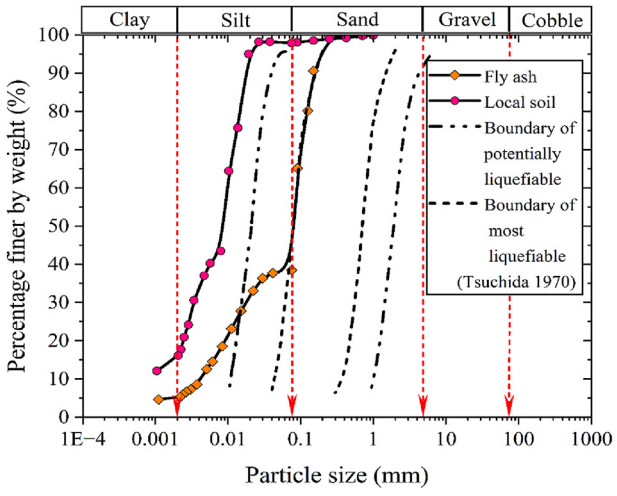

Fig. 2. Grain size distribution of soil and ash samples considered for the present study.

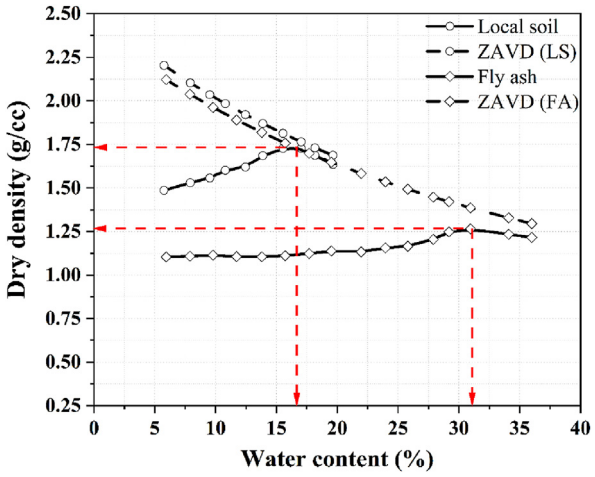

Fig. 3. Representation of standard Proctor plot of considered soil and ash samples ZAVD stands for the zero air void line.

impact of the overburden pressure. The stratified sample was prepared in two-layered forms, i.e. fly ash at the top and local soil at the bottom. The tests were conducted under consolidated undrained (CU) conditions. The sample is considered liquified (fail) when the pore water pressure becomes equal to the confining pressure.

2. Materials and methodology

2.1. Materials

The fly ash and locally available soil have been considered in the present investigation. The fly ash has been collected from Grasim Industries Private Limited, Renukoot (U·P., India). The local soil considered was collected from the Indian Institute of Technology (BHU), Varanasi campus. Since fly ash is a coal waste product, its use in bulk continues to be a major source of concern. Fly ash has often been applied over the existing soil in layers. These materials are chosen as a result in order to comprehend the dynamic

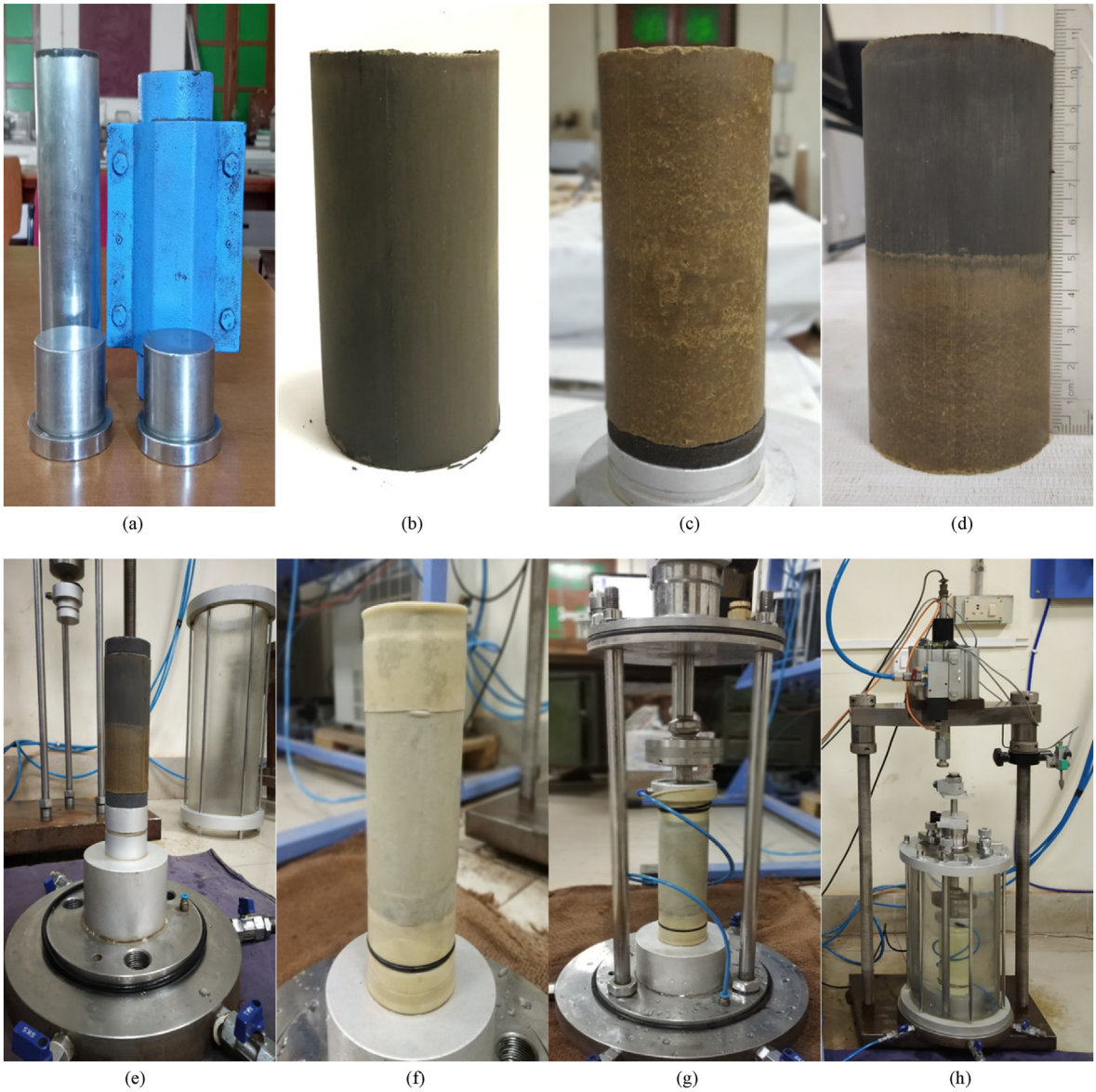

Fig. 4. Sample preparation and mounting of homogeneous/stratified soil-ash system for cyclic triaxial test.

behavior of the layered deposits. The basic geotechnical properties of fly ash and local soil are listed in Table 2. Furthermore, the plots of grain size distribution and standard Proctor test are depicted in Figs. 2 and 3 respectively. In order to eliminate the error in particle size distribution, both samples were washed thoroughly with distilled water. From Fig. 2, it can be seen that fly ash contains around 33.19% of silt size and 61.52% of fine sand size particles. Similarly, in the case of local soil, the dominance of fine to medium silt is more than that of sand and clay. The contribution of sand and clay in local soil is only about 18.23%. As per the unified soil classification system (USCS), fly ash is classified as silty sand, whereas local soil is categorized as silt of intermediate plasticity (MI). The basic geotechnical properties of the present fly ash have been taken from Ram and Mohanty (2021).

2.2. Cyclic triaxial apparatus

The selection of various methods for the determination of dynamic properties depends directly on the shear strain level. Normally, the bender element test is preferred for very small strain (<0.0001%) conditions. Similarly, the resonant column test and the cyclic triaxial test are preferred for medium to small strain (0.1%–0.0001%) and large strain (>0.1%) conditions, respectively (Ingale et al., 2017). Since the present study deals with the large strain condition, thus cyclic triaxial test has been considered. Here, a strain-controlled cyclic triaxial test has been performed under CU conditions. The tests were carried out by saturating the cylindrical specimen until Skempton's *B*-parameter becomes equal to or greater than 0.95. After that, the consolidation and shearing of the saturated specimens were done until the pore water pressure matched the effective confining pressure. The membrane stretching and mounting of the specimen within the triaxial assembly are shown in Fig. 4e–h. The cyclic triaxial setup includes a submersible load cell that can take a maximum load of ± 5 kN with an accuracy of 0.001 kN. Two linear variable displacement transducers of ±50 mm and ±10 mm have been employed for the displacement measurement with the least measurement of 0.01 mm. To measure the internal pore water pressure, a pore pressure sensor of capacity 2000 kPa has been employed (least measurement of 1 kPa). The pore pressure sensor was installed at the bottom valve opposite to the back pressure position as normally available in conventional triaxial apparatus.

2.3. Dynamic properties assessment approaches

The shear modulus and damping ratio are the two fundamental dynamic soil properties of soil that can be calculated from the hysteresis loop generated during the cyclic loading. The shear modulus is the slope of the line drawn from the origin to maximum/minimum peaks of the hysteresis loop plotted between shear stress versus shear strain. However, the damping ratio is evaluated after calculating the area of the hysteresis loop that represents the dissipation of energy and the area of the shaded portion that represents the potential energy stored, as shown in Fig. 5. In general, the soil behavior is nonlinear elastoplastic when cyclic shear strain (γ) crosses the strain range of 0.1% (>0.1%) (Ishihara, 1996). The shape of the hysteresis loop highly depends upon the shear strain level, which means the shape of the hysteresis loop changes from symmetric to asymmetric as the shear strain increases from small to large. Based on the different shapes and calculation approaches, the methods are divided into three forms such as (1) SHL, (2) ASHL, and (3) ASTM, which can be seen in Fig. 5 (Das and Chakrabortty, 2021). From Fig. 5 and Table 3, this can be observed that the determination of shear modulus requires only the secant Young's modulus both in the extension and compression sides. The secant Young's modulus is independent of the shape of the hysteresis loop rather it depends on the maximum/minimum peak of the loop. As per the definition, the damping ratio is dependent on the shape of the hysteresis loop and the

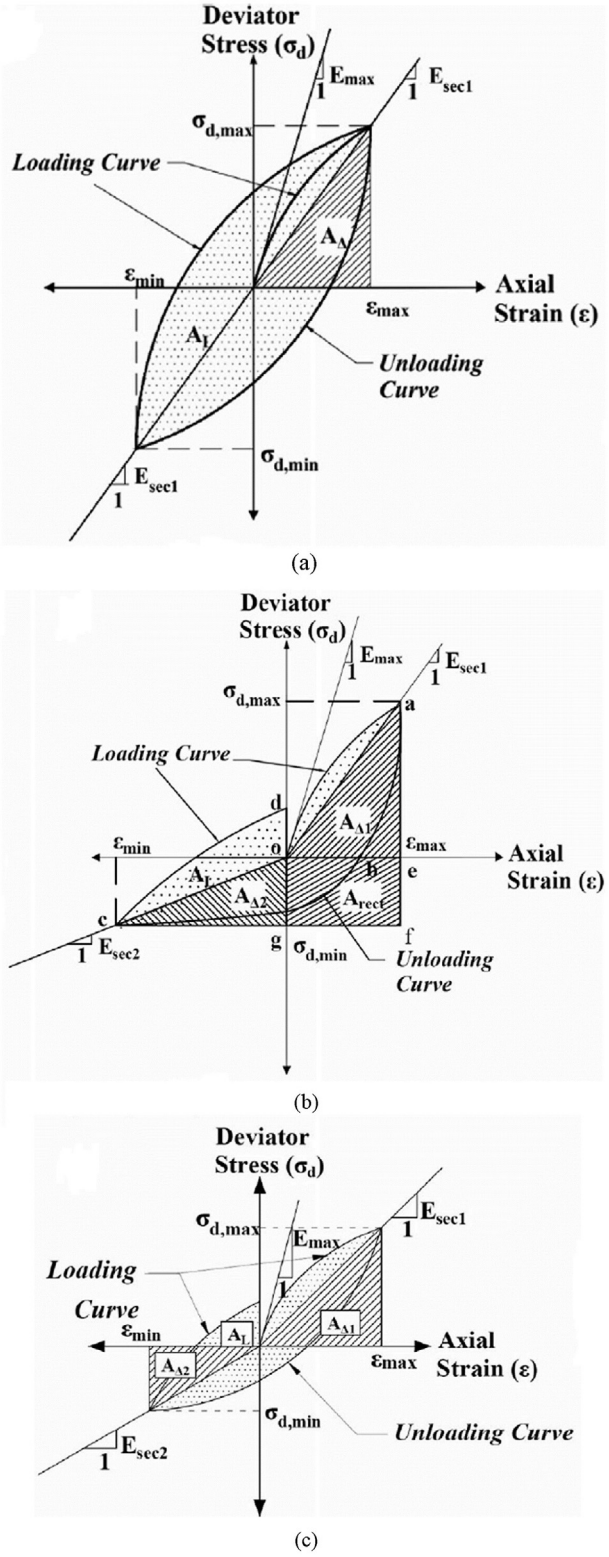

Fig. 5. Graphical illustration of various method such as (a) symmetrical hysteresis loop, (b) asymmetric hysteresis hysteresis loop, and (c) modified ASTM method for the estimation of damping ratio (Das and Chakrabortty, 2021).

Table 3
Expressions used to estimate the dynamic properties from different approaches.

Approach	Damping ratio	Secant Young's modulus, E_{sec}	Secant shear modulus, G_{sec}	Shear strain, γ
Symmetric hysteresis loop	$D_{initial} = \frac{1}{4\pi}\frac{A_L}{A_\Delta}$	$E_{sec,\ initial} = (E_{sec\ 1} + E_{sec\ 1})/2$	$G_{sec,\ initial} = \frac{E_{sec,initial}}{2(1+\upsilon)}$	$\gamma = (1+\upsilon)\varepsilon$
Asymmetric hysteresis loop	$D_{initial} = \frac{1}{\pi}\frac{A_{L(o-a-b-c-d)}}{A_{\Delta1}+A_{\Delta2}+A_{\Delta3}}$			
Modified ASTM	$D_{initial} = \frac{1}{\pi}\frac{A_L}{\left(\frac{1}{2}\sigma_{d,max}\varepsilon_{max} + \frac{1}{2}\sigma_{d,min}\varepsilon_{min}\right)/2}$			

asymmetricity at large strain influences the shape of the loop because of the variation in the peaks of the stress-strain relationship (Kokusho, 1980; Kumar et al., 2017). Kokusho (1980) first incorporated the effect of asymmetricity in damping ratio calculation which was further modified by Kumar et al. (2017) and named the ASHL approach. According to the ASTM D-3999 (1996), the SHL approach was considered a standard method, but several researchers have observed a remarkable difference in the damping ratio estimated from the ASHL method as compared to the SHL approach (Jaya et al., 2012; Kumar et al., 2017; Das and Chakrabortty, 2021). The asymmetricity plays a significant role in the accurate estimation of the damping ratio. Hence, especially in the case of large shear strain, the damping ratio must be checked with all the methods, so that the error involved can be identified. The influence of these approaches on the damping behavior of uniform and stratified soil-ash deposits has been discussed in the subsequent sections.

3. Sample preparation

Depending on the soil type, several sample preparation techniques have been employed in the past literature, i.e. pluviation through air or water, sedimentation, rodding moist/dry soil, moist tamping, and horizontal/vertical vibration technique under low and high frequencies. Mulilis et al. (1977, 1975) conducted numerous experiments considering these sample preparation techniques and found a pronounced effect of sample preparation on the cyclic strength of sand. Also, the cycle stress ratio produced by the air pluviation method was extremely low, whereas the cyclic stress ratio produced by the moist vibration provides the highest resistance. The air pluviation method is suitable for coarse-grained soil (without fines) for uniform samples while the wet pluviation method is generally used for the preparation of layered soil samples (Vasquez-Herrera and Dobry, 1989). Vaid and Negussey (1988) suggested pluviation through the air/water over moist tamping/vibration for sand without fines because the smaller velocity of fine particles leads to the segregation between coarse and fine. All the aforementioned techniques were developed for the coarse grain size particles, since it is simple to achieve the desired density due to its weight. For fine-grained soils, on the other hand, it is very difficult to obtain the desired density using any of the aforementioned procedures except the moist tamping technique. The moist tamping method is the most effective method for preparing homogenous reconstituted specimens, particularly when dealing with soil that contains fines (Ladd, 1978). The moist tamping technique has been significantly adopted by many researchers to determine the cyclic behavior of soil (having fines) (Vucetic and Dobry, 1988; Amini and Sama, 1999; Bradshaw and Baxter, 2007; Mohanty and Patra, 2016). The other available techniques (except moist tamping) need special arrangements and require a large time gap for each layer to consolidate for considered materials which mostly consist of fine-grained soil. As a result, the moist tamping approach has been taken into consideration for the sample preparation of homogeneous and layered soil-ash specimens in the current investigation. The approach involves compacting the desired amount of soil water mix in four equal proportions subjected to 25 blows each. Following that, an extruder was used to retrieve the compacted sample. Both homogeneous and stratified samples are prepared at RC of 99%, 97% and 95% of maximum dry density (MDD). The relative compaction is maintained for homogeneous soil sample preparation by looking at the dry densities and their associated moisture content from the compaction plot. In a layered soil-ash deposit, each successive layer is compacted to its dry density, which is determined by an individual compaction plot (Fig. 3). The pictorial demonstration of the uniform, and stratified soil-ash samples is depicted in Fig. 4a–d.

4. Consideration of the experimental factors

The crucial factors on which the response of soil influences during any seismic excitation are the cyclic shear strain, loading frequency, variation in density, and confining stress. In the present study, an extensive investigation into damping characteristics of uniform/stratified soil-ash deposits has been done by considering a wide range of the above-mentioned variables. For comprehensive understanding of the damping ratio of any kind of material under time-varying loading requires a profound knowledge of its response under all the aspects of variables. That is attributed to the safe and economical design of the geotechnical structures resting on it. The former researchers made a great attempt to look into the impact of many elements on the dynamic properties of soil, but further in-depth research is still needed. Dobry and Abdoun (2015) performed a strain-controlled cyclic triaxial test as well as a centrifuge model test, to determine the shear strain required to activate liquefaction. They observed that the shear strain needed in the case of silty sand was approximately 0.4%–3% under an earthquake of magnitude $M_w = 7.5$. Moreover, Tsukamoto et al. (2004) also performed a similar study based on real-time seismic data and found the initiation of liquefaction activity at 3.75% cyclic shear strain. Since the present considered materials show high dominance of silt/sand size particles. Therefore, the shear strain of 0.3%, 0.6%, 0.9%, 1.2% and 1.5% has been considered for the present study. The seismic events are random shaking movements that did not follow a uniform frequency, but in the cyclic triaxial test, a single

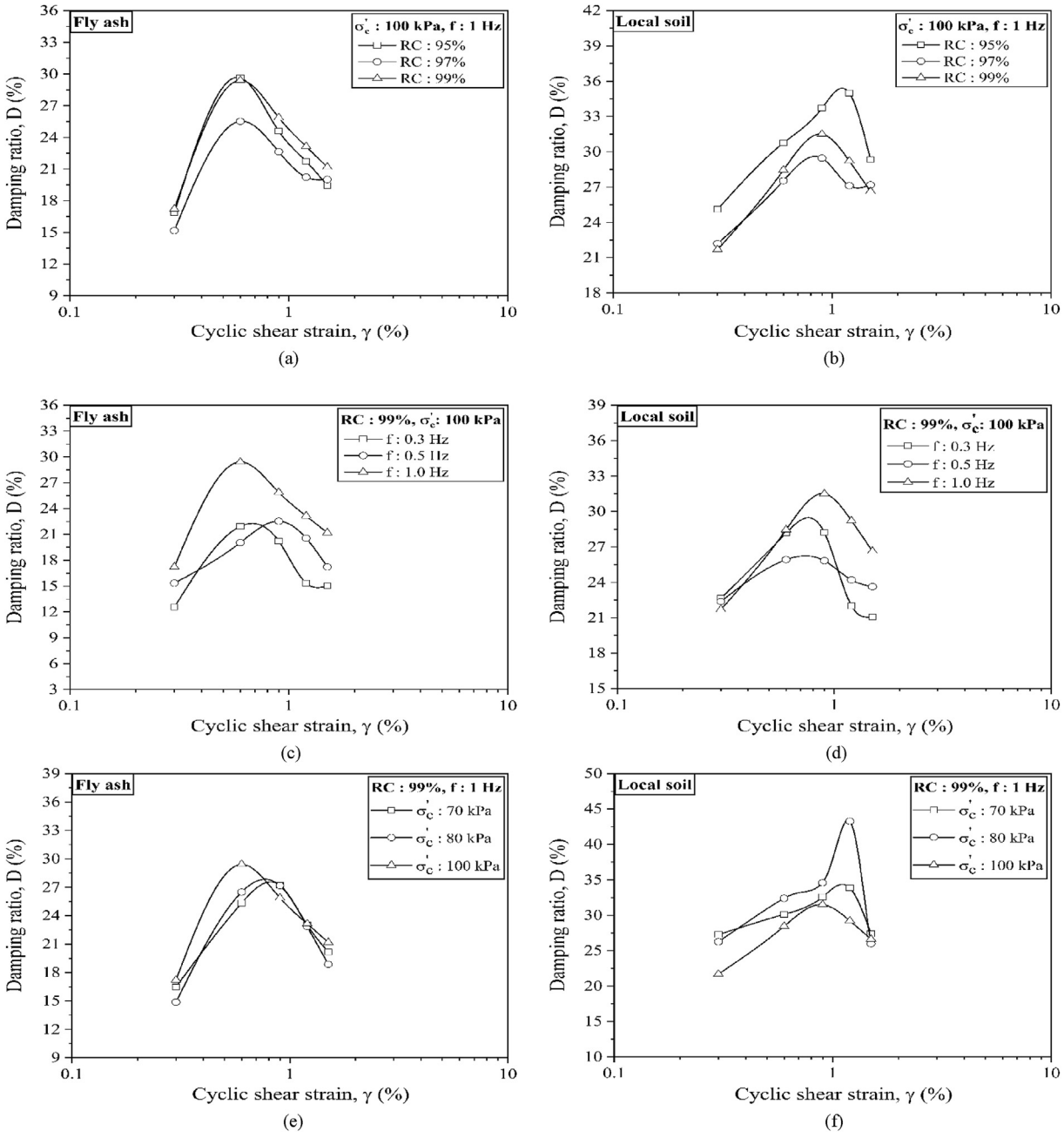

Fig. 6. Effects of various parameters on the damping ratio of fly ash (Ram and Mohanty, 2021) and local soil for large strain.

frequency of loading is considered at a particular time. In order to incorporate different loading frequencies, the cyclic loading frequency (f) of 0.3 Hz, 0.5 Hz and 1.0 Hz has been considered. Although in the case of sand, the dynamic properties are not much influenced by the loading rates (Hardin, 1965), but, Ram and Mohanty (2021) observed a significant change in the dynamic behavior of fly ash under variable loading rates. Furthermore, most of the studies usually adopt a loading frequency of 1 Hz, which can be seen in Table 1.

For sustainable functioning of fly ash applied in pavement subgrade or embankment material, it must be densified to relative compaction between 95% and 100% of MDD (ASTM-D698-12, 2012). Observing the difficulty in achieving the desired densification of fly ash, it is recommended to compact the fly ash below the optimum moisture content (OMC) (ACAA, 2003). Thus, in order to cover this range of density, the relative compaction of 95%, 97% and 99% has been chosen so that its performance under low and high densities can be analyzed. The coal ash is usually dumped in loose form and their continuous dumping results in a dump height of 10–30 m (Singh et al., 2008). Sand exhibits confining pressure between 41 and 124 kPa for the overburden height of 2–7 m (Figueroa et al., 1994). Similarly, fly ash would require an overburden height of 10–40 m to exert confining pressure between 100 and 400 kPa. But, bottom/fly ash-filled embankment up to a height of 3–5 m will generate confining pressure in the range of 10–50 kPa (Chandra et al., 2016). Hence, in order to cover the dynamic behavior of the existing height of ash pond deposits and its application in different fields of civil engineering, the confining pressure between 70 and 100 kPa has been considered here. Also, these confining pressures were frequently used by past researchers. Therefore, these

confining pressures were introduced in order to compare the current outcome with the past results more effectively.

In the cyclic triaxial test, the cylindrical specimens were subjected to an axial cyclic load that is attributed to secant Young's modulus and axial strain. The shear modulus and cyclic shear strain were determined indirectly by knowing Young's modulus and axial strain by incorporating Poisson's ratio as a conversion parameter that has been explained in Table 3. In the current investigation, samples were examined under CU conditions. According to past studies, with the increase in shear strain, the Poisson's ratio increases in the case of partially saturated soil, but in fully saturated undrained case it remains constant at 0.5 (Yokota and Konno, 1980; Sitharam et al., 2009; Kumar and Madhusudhan, 2012; Bishop and Hight, 2015). The stated reason for this is that under the saturated undrained condition, the soil behaves perfectly incompressible, which shows no volume change (Dutta, 2015). This observation has been experimentally validated by several researchers using compressive and shear wave velocities (Kokusho, 2000; Shinde and Kumar, 2022). Hence, for the determination of cyclic shear strain, Poisson's ratio of 0.5 has been adopted for both homogeneous and stratified soil-ash deposits. Similar assumptions were made by Jia and Wang (2013) for the stratified sand and silt layer. In addition, the failure of specimens was considered only when the increase in pore water pressure becomes approximately equal to the confining pressure. The development of pore water pressure was fast in fly ash, hence it takes less number of cycles to fail than that of the local and stratified arrangement. In the case of fly ash, the number of cycles was between 300 and 500 (approximately), whereas for local soil, it was observed in the range of 600–800 (approximately). However, stratified soil takes an intermediate number of cycles, i.e. between fly ash and local soil.

5. Results and discussion

Based on past earthquake studies, Tsuchida (1970) reviewed the particle size distribution of liquefied/non-liquefied soils and suggested a grain size distribution curve for most/potentially liquefiable soil. The fly ash and local soil have also been checked for their liquefaction susceptibility through this distribution curve, as shown in Fig. 2. About more than 50% of fly ash particles are coinciding with the boundary of most liquefiable soil and 17% of the particles are falling between these two boundaries (most likely/likely to liquefy). On the other hand, local soil has almost < 5% of particles in the boundary of most liquefiable and potentially liquefiable soil. Since silt particles are predominant in the local soil and after sandy soil fraction, silt-size particles are more prone to liquefaction. Hence, according to Tsuchida's chart, fly ash can be treated as partially liquefiable whereas local soil can be considered non-liquefiable soil. Therefore, the considered materials, i.e. fly ash and local soil, need to be studied thoroughly under dynamic loading conditions to understand their dynamic responses. As the damping characteristics of the material significantly affect the dynamic responses, an attempt is made to investigate the damping behavior of the uniform and stratified soil-ash specimens under dynamic loading conditions. A detailed discussion on the damping behavior of uniform and stratified soil-ash samples is reported in the subsequent sections.

5.1. Discussion on the damping response of uniform soil and fly ash specimens

This section presents the damping (D) response of uniform fly ash and local soil samples under the influences of relative compaction, frequency, and confining pressure. In order to estimate the damping behavior of uniform soil and ash samples, the SHL approach is employed. The variation of damping ratio with the cyclic shear strain of both the materials considering all the variables

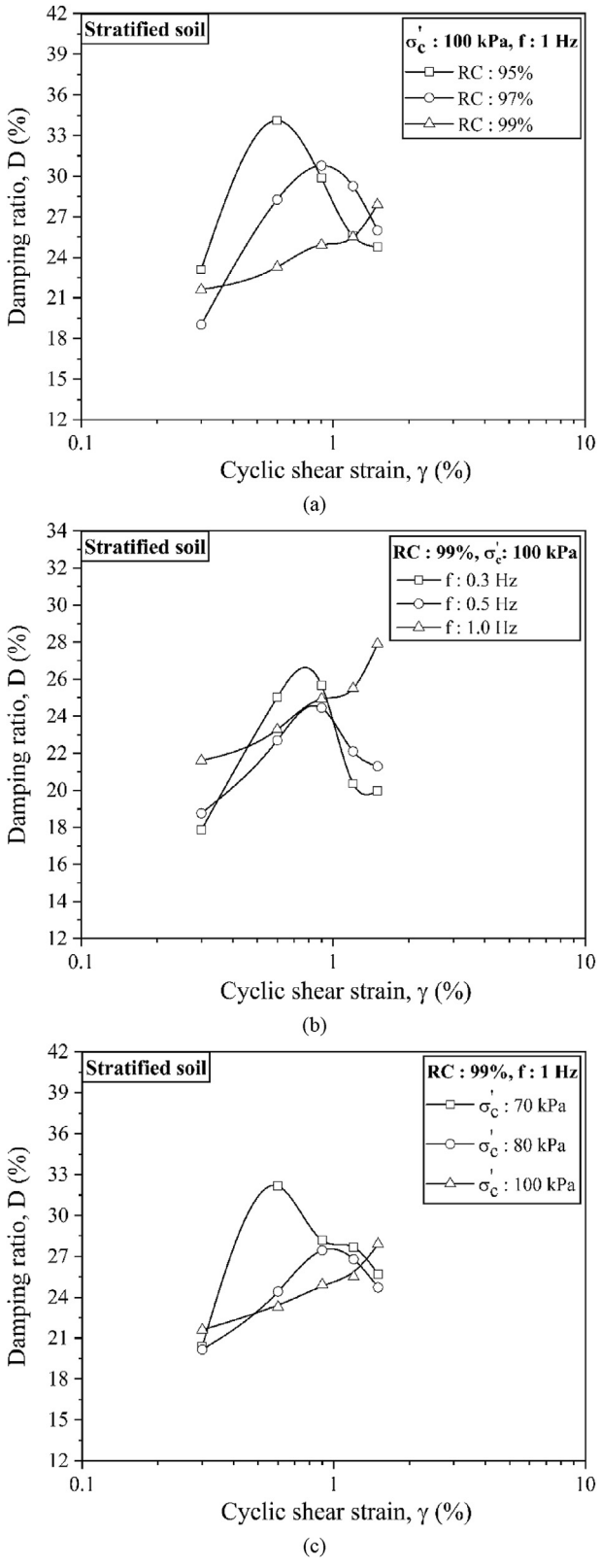

Fig. 7. Variations of damping ratio of stratified soil-ash samples considering all influencing parameters.

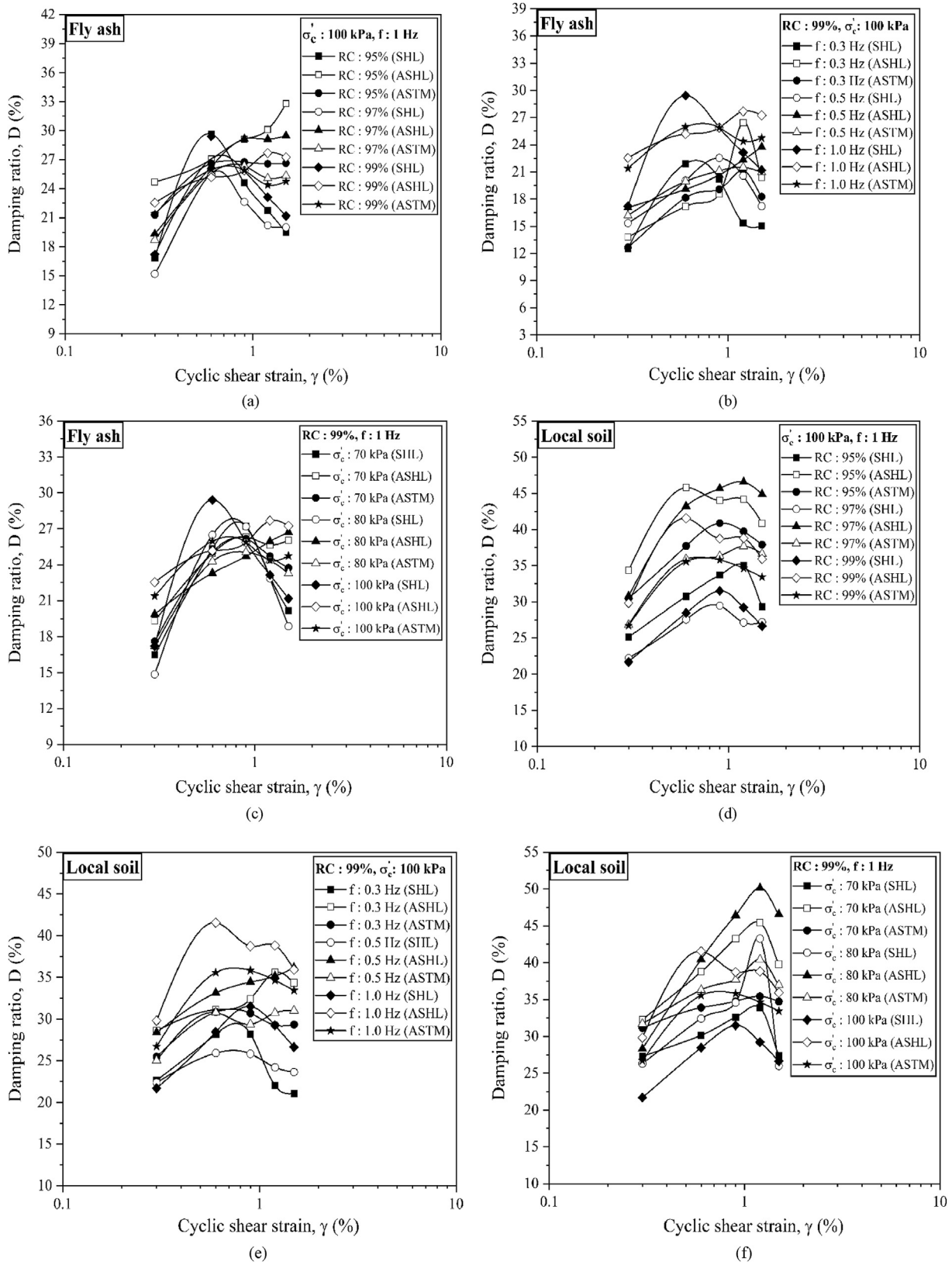

Fig. 8. Graphical representation of damping ratio of fly ash and local soil evaluated using SHL, ASHL and ASTM methods.

is shown in Fig. 6. From the figure, it can be seen that fly ash shows a continuous incremental trend of damping ratio till 0.6% of shear strain after that it decreases consistently with the increase in shear strain. However, the damping ratio of local soil shows an incremental trend up to 1% or 1.2% shear strain, then attains a peak and subsequently decreases. Considering the relative compaction effect, both materials exhibits high damping value for lower density except at 99% density. In general, highly compacted soil dissipates less energy under dynamic loading which ultimately results in a low damping ratio value. Similarly, for the evaluation of the frequency effect, the samples were prepared at 99% of RC and that have been subjected to an effective confining pressure of 100 kPa. From Fig. 6, this can be observed that both material shows a high damping value for the high frequency of loading. The confining pressure effect has been checked considering the confining pressure of 70 kPa, 80 kPa and 100 kPa. No significant difference in damping value has been observed under different confining pressures for both of the materials (fly ash and local soil). From the above discussion, this can be inferred that the damping ratio of uniform soil shows a remarkable dependency on relative compaction, frequency of loading, and cyclic shear strain, and shows the least influence on confining pressure. In past studies, almost every material expressed decreasing trend of shear modulus and a corresponding increasing trend of damping ratio with an increase in shear strain. However, fly ash and local soil show a decreasing trend after peak. Thus in order to determine the accurate damping behavior, additional approaches (ASHL and ASTM) were incorporated here that have been explained in the subsequent sections.

5.2. Discussion on the damping response of the stratified soil-ash system

Similar to uniform fly ash and local soil samples, the damping behavior of stratified soil-ash specimens has also been evaluated incorporating the influences of relative compaction, loading frequency, and confining pressure. The variation of the damping ratio with cyclic shear strain considering all the above-mentioned variables is shown in Fig. 7. This damping analysis was also carried out using the SHL approach. Here, in the relative compaction study, the stratified soil-ash specimens show an inverse relation between damping values and density under low shear strain. The damping nature is primarily attributed to the slippage of particles and rearrangements of particles in soil (Fahoum et al., 1996). The probability of slippage and particle rearrangements is greater in low-density specimens than in high-density specimens due to the availability of high voids, which eventually results in higher damping value. The difference in the damping ratio gets minimized as the shear strain increases (Fig. 7a). In this arrangement, remarkable changes in the damping ratio value have been observed under the influence of loading frequency, as shown in Fig. 7b. As compared with the uniform soil, the stratified soil-ash arrangements show considerable variation in damping ratio with the increase in confining pressure. The trend of the damping ratio profile with cyclic shear strain is similar to homogeneous soil and it also attains its peak around 1% of shear strain.

From Fig. 6, this can be inferred that the peak value of damping ratio of the fly ash varies between 0.6% and 0.9% of shear strain, however, the local soil shows a peak between 0.8% and 1.2% of shear strain. On the other hand, the stratified soil exhibits a wide range of damping ratio's peak variation, i.e. in the range of 0.6%–1% of shear strain that can be seen in Fig. 7. The maximum damping ratio of fly ash is always lower than the maximum damping ratio of local soil. Whereas the maximum damping ratio of stratified soil always falls in between the damping ratio of fly ash and local soil. This is due to the combined interactive behavior of fly ash and local soil composite. The percentage variation of damping ratio of fly ash varies between 100% and 150% and local soil varies in the range of 52%–65% as compared to their minimum values. The fly ash shows a wide range of percentage variation of damping ratio, i.e. 100%–150%. Similarly, local soil depicts a narrow range of percentage variation of damping ratio, i.e. 52%–65%. From the above

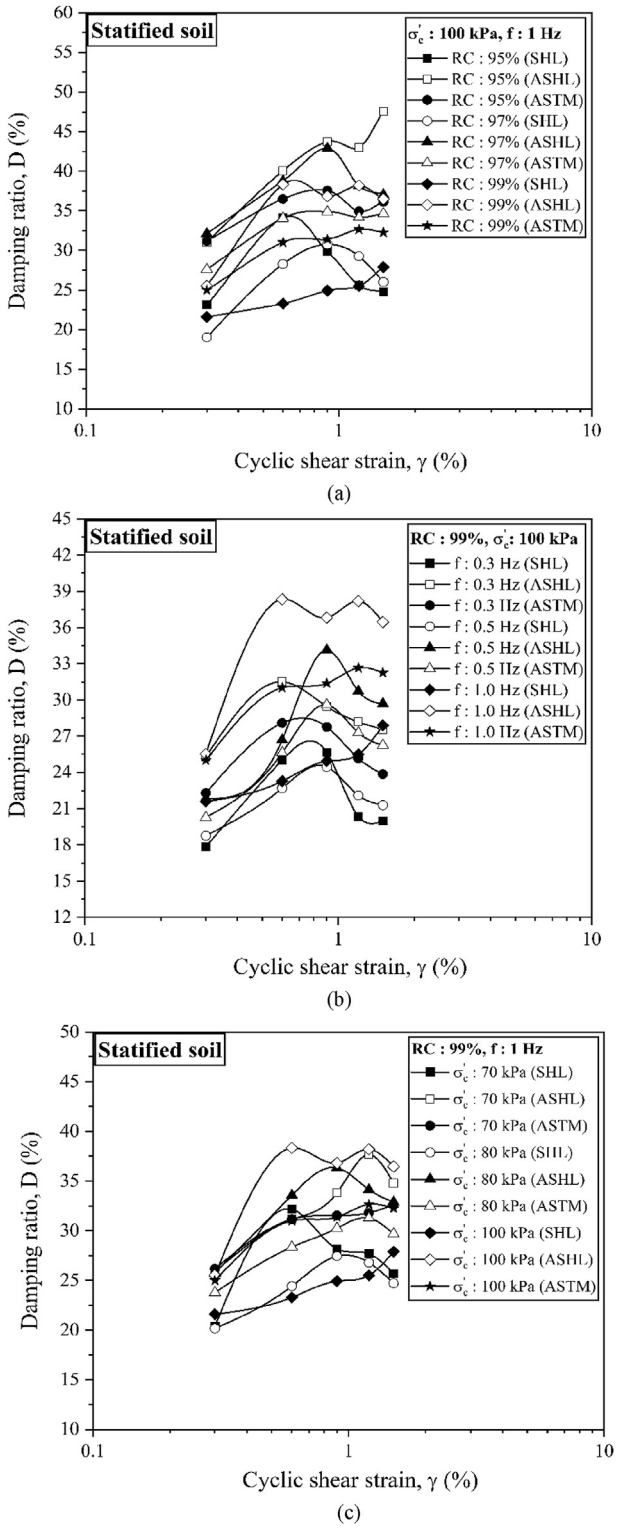

Fig. 9. Graphical representation of damping ratio of stratified soil-ash samples evaluated using SHL, ASHL and ASTM methods.

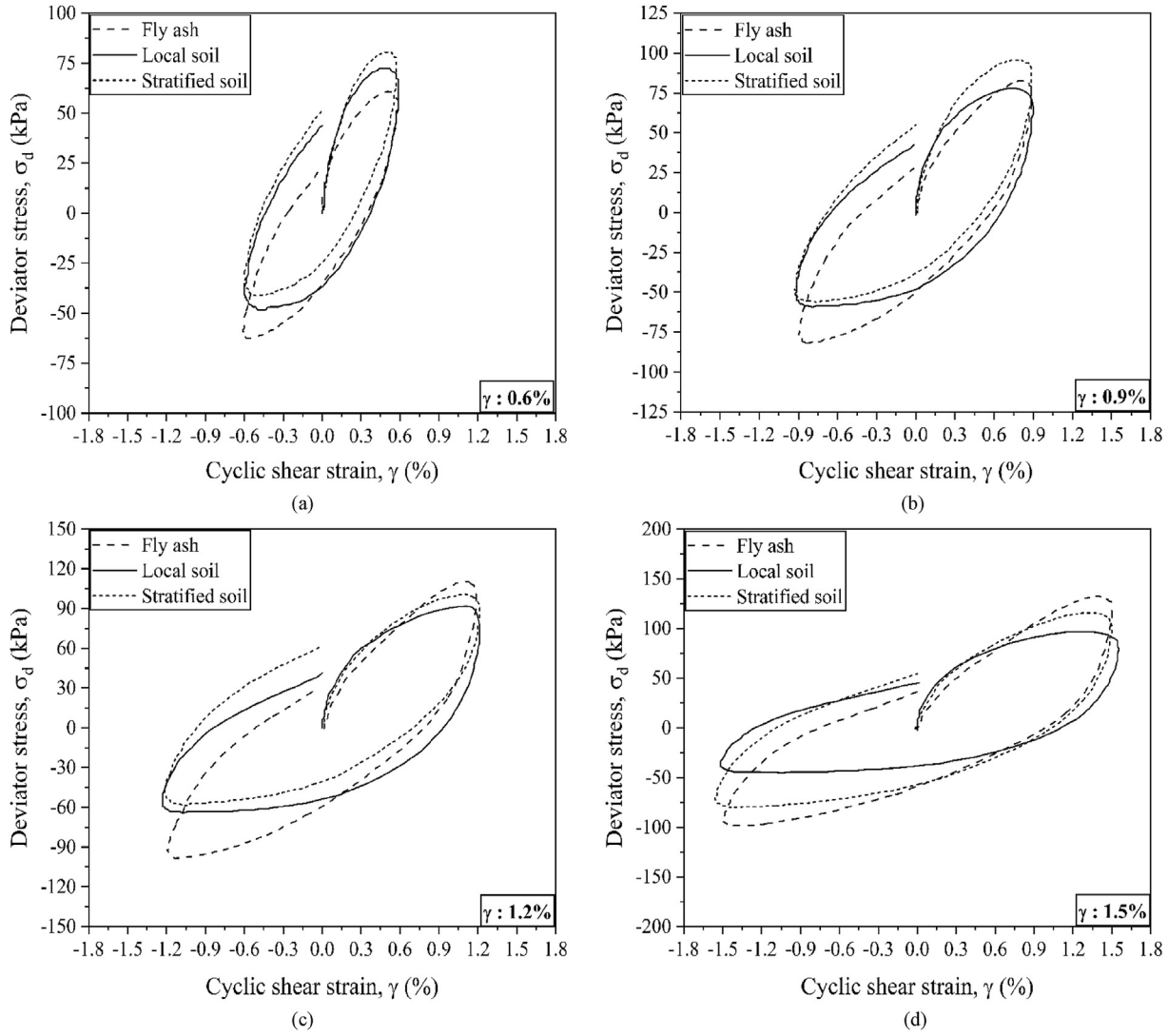

Fig. 10. Asymmetricity of hysteresis loop at 0th cycle position under different cyclic shear strains for uniform and stratified soil-ash samples.

discussion, this can be concluded that the profile between the damping ratio versus shear strain is similar for both the homogeneous and stratified soils, but the peak of damping ratio is observed to be varied in a wide range for stratified soil. Also, the development of excess pore pressure in the stratified soil is fast as compared to the local soil due to the high permeability of fly ash.

5.3. Identification of an appropriate method for damping ratio

In the present study, all the experimental studies were carried out by employing cyclic triaxial apparatus that is generally used for large strain dynamic investigation of soil. Normally, an SHL approach was adopted for the estimation of damping ratio in past studies. The SHL approach is not reliable, especially in the case of large shear strain because under large strain the shape of the hysteresis loop becomes unsymmetrical which results in under/overestimation of the damping ratio value. Hence, in order to diminish the influence of asymmetricity in the magnitude of damping ratio, two different approaches such as ASHL and ASTM approaches have been developed. The fundamental of these approaches has already been illustrated in the above-mentioned sections and their graphical and analytical equations are reported in Fig. 5 and Table 3. Here, an attempt has also been made to determine the effect of asymmetricity on the damping ratio of uniform and stratified soil-ash systems under large strain conditions. The graphical representation of the damping ratio obtained from all these approaches for uniform and stratified soil-ash systems are depicted in Fig. 8 and9, respectively.

In Fig. 8, the impacts of all the variables (RC, CP and f) on the damping ratio computed through the above-mentioned approaches for both uniform materials (fly ash and local soil) are reported. The SHL approach follows an identical profile of damping ratio versus shear strain plot for all the variables as compared with the other two approaches. Whereas the ASHL approach shows an increasing trend of damping profile as observed in past literature. Among all the approaches, the ASHL approach gives a higher damping ratio value, followed by the ASTM and then the SHL approach for fly ash. The high-density sample provides a low damping value irrespective of different approaches (Fig. 8a). A similar trend of frequency effect is observed in the ASHL and ASTM methods as in the SHL approach (Fig. 8b). The damping ratio of fly ash samples is not much affected by the confining pressure changes as seen in Fig. 8c. In the case of local soil, the ASHL approach gives higher damping values as compared with the SHL and ASTM

approaches. However, the ASTM approach is not showing much difference in damping value and appears always in between the ASHL and SHL approaches. Similar kind of trends of variables in damping value has been observed in local soil as witnessed for fly ash. Hence, from the above discussion, this can be noticed that the SHL approach underestimates the damping behavior of fly ash and local soil. The ASHL approach represents the same kind of trend that had been observed in past studies for similar materials. On the other hand, the ASTM approach does not show significant variation in damping value and also gives more or less the same value with the increase in shear strain.

The damping characteristics of the stratified soil-ash sample have been determined to assess the significance of various approaches and their impact on the influencing variables. The comparison of each approach considering the effect of all the influencing variables is presented in Fig. 9. The stratified soil-ash also exhibits a higher damping value in the case of the ASHL approach and a lower value for the SHL approach. From Figs. 8 and 9, this can be observed that the damping profile evaluated from each method follows an increasing curve that reaches the peak and then decreases. The maximum damping ratio was ascertained at nearly 1% of shear strain which was also discovered at the same

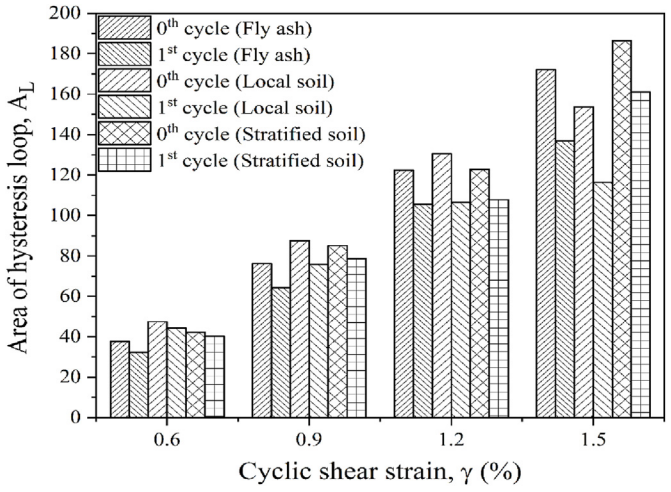

Fig. 12. Bar distribution of area of hysteresis loop plotted against 0th and 1st cycle positions.

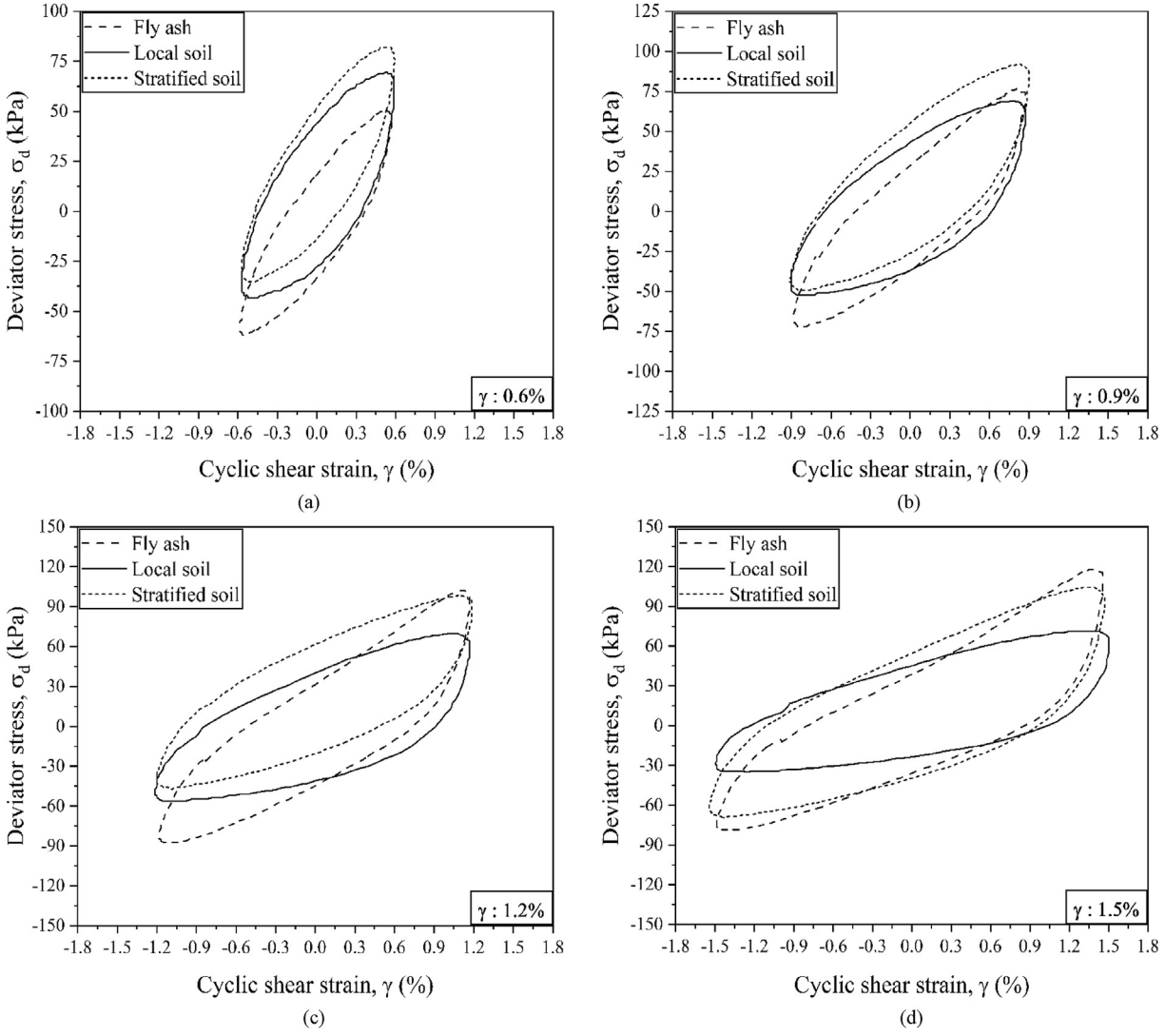

Fig. 11. Asymmetricity of hysteresis loop at 1st cycle position under different cyclic shear strains for uniform and stratified soil-ash samples.

Table 4
Representation of damping ratio estimated using different approaches under various cycles at different relative compaction.

MDD (%)	Shear strain (%)	Fly ash						Local soil						Stratified soil					
		SHL		ASHL		ASTM		SHL		ASHL		ASTM		SHL		ASHL		ASTM	
		0th cycle	1st cycle	0th cycle	1st cycle	0th cycle	1st cycle	0th cycle	1st cycle	0th cycle	1st cycle	0th cycle	1st cycle	0th cycle	1st cycle	0th cycle	1st cycle	0th cycle	1st cycle
95	0.3	16.84	17.82	24.69	23.32	21.3	20.54	25.1	23.65	34.35	34.11	30.46	28.59	23.11	28.58	31.06	29.43	31.19	28.69
	0.6	29.65	26.27	27.05	24.74	26.62	24.77	30.75	28.6	45.79	45.81	37.72	37.53	34.11	28.59	40.05	38.2	36.49	33.88
	0.9	24.59	21.03	29.12	27.54	26.75	24.5	33.7	32.46	44.02	42.92	40.88	39.7	29.84	27.9	43.72	43.14	37.54	35.93
	1.2	21.72	18.98	30.1	29.11	26.58	24.64	34.99	32.31	44.15	41.52	39.74	37.52	25.57	24.49	42.99	44.67	34.94	34.88
	1.5	19.46	16.86	32.79	32.59	26.63	24.77	29.33	30.91	40.88	40.05	37.9	36.79	24.76	24.32	47.56	45.88	36.13	35.35
97	0.3	15.17	15.91	19.33	18.96	18.7	17.32	22.2	21.75	30.8	27.14	26.82	25.24	19.02	20.51	32.11	30.63	27.61	25.78
	0.6	25.53	23.55	26.3	25.74	25.6	24.77	27.54	26.02	43.24	41.48	35.93	35.21	28.27	25.12	38.78	38.28	34.06	32.59
	0.9	22.64	19.59	29.14	28.08	26.35	24.33	29.46	29.65	45.67	44.38	36.34	36.1	30.78	29.41	42.88	42.88	34.88	34.47
	1.2	20.22	17.05	29.12	27.01	25.08	23.12	27.13	28.41	46.58	43.68	37.69	37.05	29.26	27.87	38.15	37.97	34.17	33.43
	1.5	20.02	17.52	29.48	28.25	25.34	23.41	27.19	28.67	44.88	42.3	36.63	36.52	26	24.02	37.02	35.11	34.63	33.25
99	0.3	17.21	17.85	22.55	19.5	21.39	18.78	21.69	20.37	29.81	27.13	26.71	25.56	21.6	19.76	25.53	23.72	25	23.51
	0.6	29.41	27.60	25.17	23.24	25.96	24.29	28.45	26.85	41.56	38.33	35.57	33.77	23.28	20.67	38.33	37.25	31.01	29.54
	0.9	25.88	23.68	25.88	24.73	25.88	24.23	31.5	32.02	38.73	38.79	35.80	35.7	24.93	23.71	36.82	36.8	31.39	30.96
	1.2	23.14	21.86	27.68	26.52	24.38	23.27	29.22	33.18	38.81	38.72	34.63	36.12	25.5	22.97	38.19	38.22	32.65	31.3
	1.5	21.19	19.66	27.25	26.16	24.74	23.3	26.63	27.16	35.92	34.23	33.43	31.59	27.9	26.39	36.46	35.33	32.25	31.06

shear strain by Matasović and Vucetic (1993) and Kumar et al. (2018). Kiku and Yoshida (2000) and Mashiri (2014) noticed the peak damping at 0.1% and 0.23% of shear strain respectively. The reason behind the drop in damping ratio is due to the sudden and significant rise in pore water pressure, particularly at large strain that results in frictional energy loss in the soil skeleton (Mashiri, 2014). According to Matasović and Vucetic (1993), the decrement in damping value is due to the 'S' shaping of shear stress versus shear strain curve that is attributed to the dilative behavior of soil particles at large strain. After analyzing Figs. 8 and 9, numerous conclusions can be drawn: (1) the SHL approach underestimates the damping property of uniform and stratified samples; (2) the ASHL approach would be a better option for the precise estimation of the damping ratio because this method is in good agreement with the past reported results, i.e. damping estimated from SHL is always lower than the damping estimated by ASHL approach; (3) the ASTM approach is not well defined as compared with the ASHL approach. The asymmetricity is predominantly attributed to the first, third and fourth quadrants of the hysteresis loop plot between deviator stress versus axial strain. The SHL approach just takes into account the first quadrant whereas the ASTM approach takes the first and third quadrants for the estimation of damping ratio. The ASHL approach is the only approach that considered all the quadrants, that is significantly involved in the asymmetricity of the hysteresis loop which can be seen in Fig. 5. Hence, considering the formulation and area of loop involved, the ASHL approach can be contemplated as more realistic/practical compared with other approaches. The average variation of the SHL and ASHL approaches is around 20%–60%, which is similar to the past reported studies (Kumar et al., 2017; Das and Chakrabortty, 2021). Hence, especially for large-strain dynamic characterization, the damping ratio must be evaluated using the method that considers asymmetricity in its calculation (i.e. the ASHL approach).

5.4. Assessment of the influence of cycle position on damping ratio

Conventionally, the damping ratio is estimated by implementing the 0th position cycle hysteresis loop. Nevertheless, the 0th position cycle may comprise flaws due to the improper contact between the top pedestal and specimen or due to the discontinuity between the start and end points of the hysteresis loop. The cycle position of the 0th and 1st cycles has been considered to identify the variation in the damping property of the uniform and stratified soil-ash deposits owing to cycle position. The change in the shape

Table 5
Representation of damping ratio estimated using different approaches under various cycles at different confining pressure.

Confining pressure (kPa)	Shear strain (%)	Fly ash						Local soil						Stratified soil					
		SHL		ASHL		ASTM		SHL		ASHL		ASTM		SHL		ASHL		ASTM	
		0th cycle	1st cycle	0th cycle	1st cycle	0th cycle	1st cycle	0th cycle	1st cycle	0th cycle	1st cycle	0th cycle	1st cycle	0th cycle	1st cycle	0th cycle	1st cycle	0th cycle	1st cycle
70	0.3	16.48	15.49	19.32	18.51	17.61	16.31	27.27	29.52	32.26	32.75	31.14	30.53	20.4	22.83	25.89	24.24	26.18	23.27
	0.6	25.33	23.58	24.93	23.73	25.06	23.88	30.13	29.01	38.74	38.64	33.89	33.82	32.17	29.14	31.14	29.47	31.15	30.15
	0.9	27.21	23.53	26.33	25.23	26.17	24.37	32.59	30.92	43.26	41.94	34.76	33.98	28.16	27.09	33.81	33.37	31.53	30.52
	1.2	23.01	21.15	25.65	24.05	24.7	23	33.87	31.51	45.41	43.66	35.43	34.89	27.67	25.48	37.65	37.11	31.79	30.64
	1.5	20.16	18.15	26.03	24.72	23.734	22	27.35	27.11	39.78	38.3	34.72	33.93	25.69	24.17	34.8	33.39	32.64	31.34
80	0.3	14.86	16.18	19.88	18.51	17.22	16.59	26.28	25.49	28.3	28.29	31.71	32.26	20.16	18.94	25.75	24.94	23.78	22.39
	0.6	26.5	25.78	23.3	22.77	24.28	23.69	32.4	29.98	40.43	38.89	36.3	34.66	24.42	22.81	33.57	31.49	28.36	27.75
	0.9	27.18	25.15	24.72	22.98	25.05	23.24	34.59	33.59	46.43	46.51	37.71	37.81	27.43	26.55	36.34	35.22	30.24	30.06
	1.2	22.86	21.19	25.95	24.73	24.36	23.07	43.26	40.98	50.14	49.07	40.43	37.91	26.79	25.61	34.14	34.12	31.28	30.61
	1.5	18.87	17.42	26.72	25.85	23.29	22.04	26	25.83	46.55	46.05	36.99	36.52	24.71	23.63	32.88	32.51	29.69	29.32
100	0.3	17.21	17.85	22.55	19.50	21.39	18.78	21.68	20.37	29.81	27.12	26.71	25.56	21.6	19.76	25.53	23.73	25	23.51
	0.6	29.41	27.6	25.17	23.24	25.96	24.29	28.45	26.85	41.56	38.33	35.57	33.77	23.28	20.67	38.33	37.25	31.01	29.54
	0.9	25.88	23.68	25.88	24.73	25.88	24.23	31.5	32.02	38.73	38.79	35.8	35.7	24.93	23.71	36.82	36.8	31.39	30.96
	1.2	23.14	21.86	27.68	26.52	24.38	23.27	29.22	33.18	38.81	38.72	34.63	36.12	25.5	22.97	38.19	38.22	32.65	31.3
	1.5	21.19	19.66	27.25	26.16	24.74	23.3	26.63	27.16	35.92	34.23	33.43	31.59	27.9	26.39	36.46	35.33	32.25	31.06

Table 6
Representation of damping ratio estimated using different approaches under various cycles at different loading frequency.

Frequency (Hz)	Shear strain (%)	Fly ash						Local soil						Stratified soil					
		SHL		ASHL		ASTM		SHL		ASHL		ASTM		SHL		ASHL		ASTM	
		0th cycle	1st cycle	0th cycle	1st cycle	0th cycle	1st cycle	0th cycle	1st cycle	0th cycle	1st cycle	0th cycle	1st cycle	0th cycle	1st cycle	0th cycle	1st cycle	0th cycle	1st cycle
0.3	0.3	12.55	10.66	13.79	12.48	12.64	12.2	22.64	20.38	28.58	27.75	25.46	24.51	17.86	15.85	25.3	24.86	22.3	21.11
	0.6	21.93	19.83	17.19	15.28	18.15	16.37	28.17	27.62	31.1	27.62	30.82	27.62	25.02	16.84	31.51	28.56	28.09	23.85
	0.9	20.21	17.06	18.57	16.52	19.08	16.59	28.21	27.71	32.38	30.68	30.69	28.97	25.66	22.67	29.45	28.13	27.76	25.77
	1.2	15.34	12.22	26.43	26.28	21.13	18.85	22	21.8	35.59	35.37	29.25	29.03	20.36	18.48	28.17	27.14	25.15	23.63
	1.5	15.03	12.45	20.38	18.73	18.27	16.03	21.07	20.2	34.33	32.3	29.32	28.36	19.98	17.96	27.55	26.85	23.85	22.51
0.5	0.3	15.34	13.47	17.08	16.47	16.17	14.65	22.37	20.38	28.37	27.69	25.02	24.62	18.76	16.8	21.86	19.9	20.28	19.03
	0.6	20.03	18.01	19.08	16.98	19.95	17.65	25.91	24.83	33.13	32.41	30.76	29.63	22.69	21.9	26.68	25.16	25.61	23.97
	0.9	22.53	19.25	20.66	18.23	21.11	18.44	25.82	24.34	34.43	33.78	29.35	27.89	24.45	22.95	34.14	32.87	29.59	28.2
	1.2	20.55	17.25	22.31	19.95	21.51	18.81	24.2	23.71	35.13	34.33	30.73	29.97	22.1	20.74	30.72	29.24	27.27	25.81
	1.5	17.21	14.35	23.74	21.79	20.96	18.49	23.62	22.99	36.15	34.64	31.02	29.79	21.29	19.5	29.69	28.63	26.24	24.76
1	0.3	17.21	17.85	22.55	19.50	21.39	18.78	21.68	20.37	29.81	27.13	26.71	25.56	21.6	19.76	25.53	23.73	25	23.51
	0.6	29.41	27.6	25.17	23.24	25.96	24.29	28.45	26.85	41.56	38.33	35.57	33.77	23.28	20.67	38.33	37.25	31.01	29.54
	0.9	25.88	23.68	25.88	24.73	25.88	24.23	31.5	32.02	38.73	38.79	35.8	35.7	24.93	23.71	36.82	36.8	31.39	30.96
	1.2	23.14	21.86	27.68	26.52	24.38	23.27	29.22	33.18	38.81	38.72	34.63	36.12	25.5	22.97	38.19	38.22	32.65	31.3
	1.5	21.19	19.66	27.25	26.16	24.74	23.3	26.63	27.16	35.92	34.23	33.43	31.59	27.9	26.39	36.46	35.33	32.25	31.06

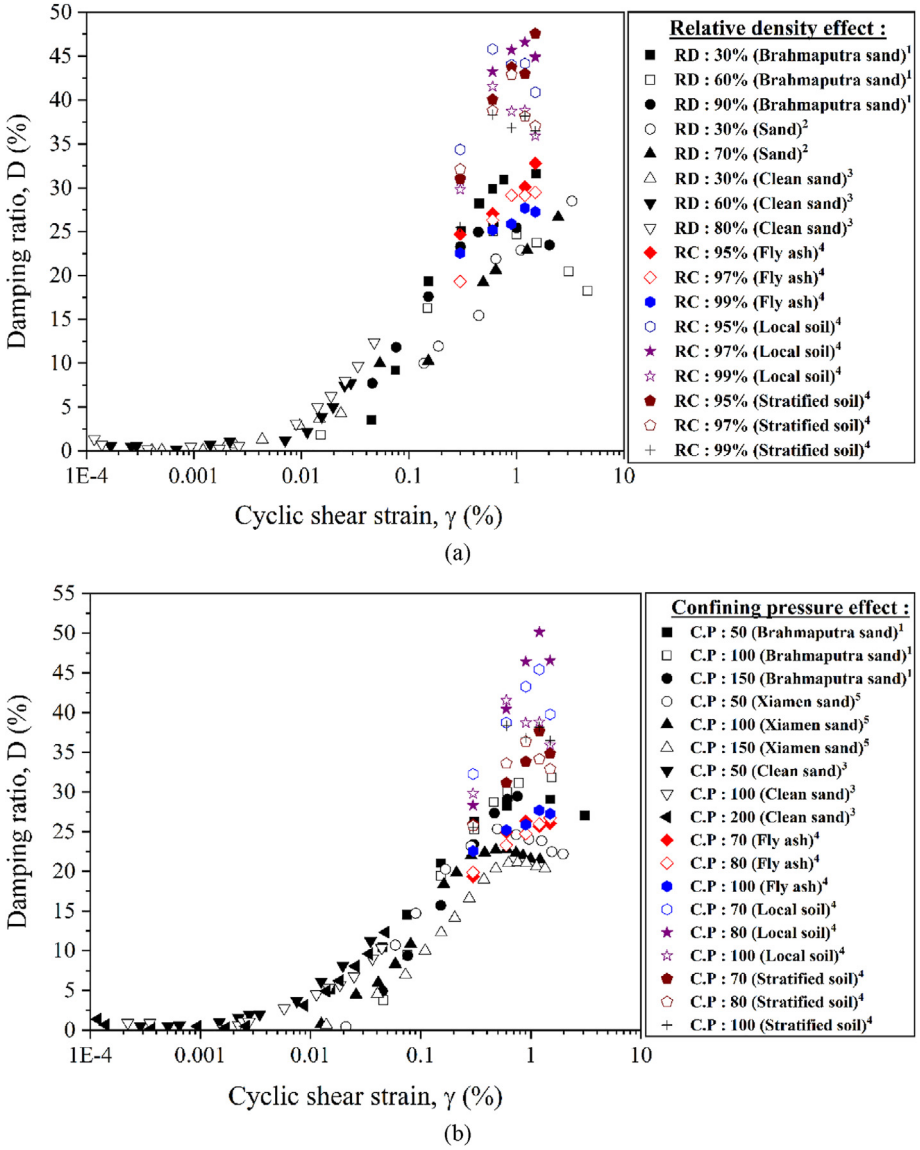

Fig. 13. Assessment of damping characteristics of present study results with different types of soil considering the effect of relative compaction and confining pressure ([1] Kumar et al., 2014; [2] Ravishankar and Sitharam, 2005; [3] Mog and Anbazhagan, 2022; [4] Present study; [5] Li et al., 2020).

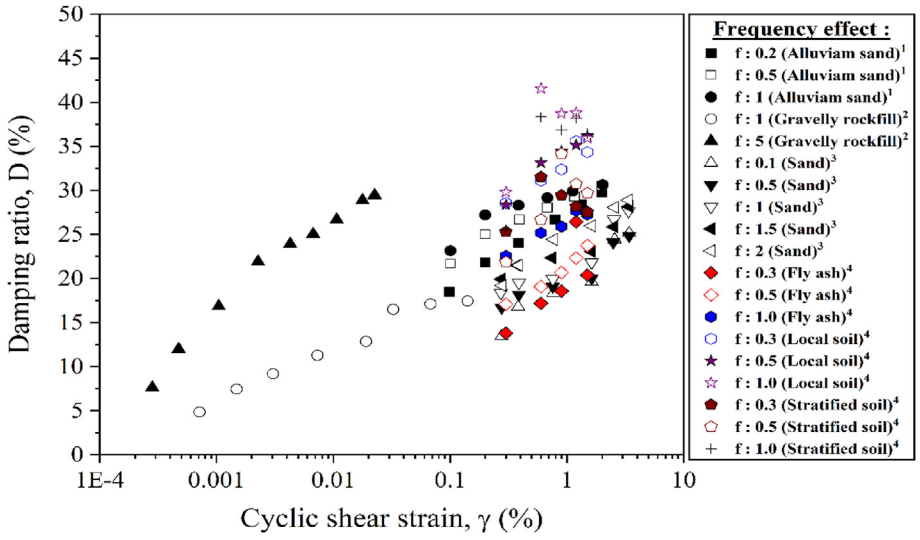

Fig. 14. Assessment of damping ratio of present study results with different types of soil under the influence of frequency of loading ([1] Das and Chakrabortty, 2021; [2] Araei et al., 2012; [3] Ravishankar and Sitharam, 2005; [4] Present study).

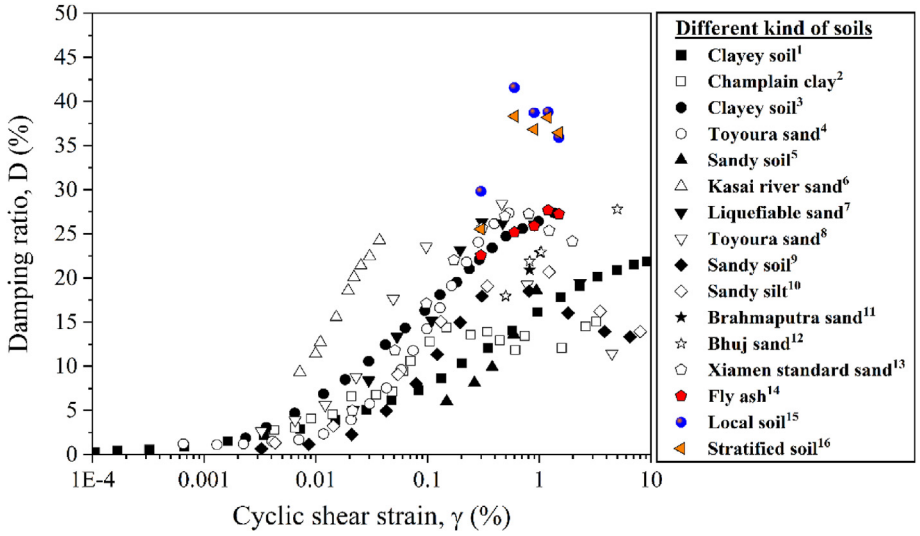

Fig. 15. Comparison of damping ratio of present study results with different types of soil ([1] Amir-Faryar et al., 2017; [2] Chehat et al., 2019; [3] Vucetic and Dobry, 1991; [4] Kokusho, 1980; [5] Hanumantharao and Ramana, 2008; [6] Chattaraj and Sengupta, 2016; [7] Matasovic and Vucetic, 1993; [8] Kiku and Yoshida, 2000; [9] Chiaradonna et al., 2015; [10] Pagliaroli et al., 2018; 11 Kumar et al., 2014; [12] Govindaraju et al., 2004; [13] Li et al., 2020; [14, 15, 16] Present study).

of the hysteresis loop under the influence of shear strain (0.6%–1.5%) for both cycles (0th and 1st) is shown in Figs. 10 and 11. A remarkable change in the shape of the hysteresis loop can be observed from the figures, especially for the strains of 1.2% and 1.5%. The enclosed area of the hysteresis loop rises as the shear strain increases, resulting in a higher damping ratio under high-strain values. Given that these tests are strain-controlled, low resistance will emerge under low-strain cyclic loading, which will result in a small-size hysteresis loop. However, in the case of high-strain loading, high resistance will be experienced by the sample that ultimately exhibits an increase in the length and width of the hysteresis loop. This increase in the size of the hysteresis loop can be witnessed in Figs. 10 and 11. Several researchers in the past studies have recognized a similar kind of increment in damping ratio with the increase in shear strain (Kokusho et al., 1982; Dammala et al., 2017, 2019; Kumar et al., 2017; Das and Chakrabortty, 2021). The reduction in deviator stress from the 0th cycle to the 1st cycle is approximately 10% for all the cases of uniform and stratified soil-ash deposits. This drop in deviatoric stress increases by approximately 13%–23% as the shear strain reaches a large strain that can be deduced from Figs. 10 and 11. To understand the reduction phenomenon of the hysteresis loop, the area of the hysteresis loop (A_L) corresponding to each shear strain for the entire soil and ash sample has been expressed in the form of a bar chart as shown in Fig. 12. The same figure shows that the influence of cycle position is not remarkable for low shear strain, but for high strain, this difference in A_L is pronounced. The damping ratio evaluated from the SHL, ASHL and ASTM methods under the 0th and 1st cycles considering relative compaction, confining pressure and frequency is enumerated in Tables 4–6, respectively. After analyzing the damping ratio obtained for various relative compactions, this can be inferred that the fly ash and stratified soil-ash indicate a high difference in the 0th and 1st cycles for the SHL approach followed by the ASTM approach and then the ASHL approach. The variation in the damping ratio between the 0th and 1st cycles estimated from the SHL, ASHL, and ASTM approaches are

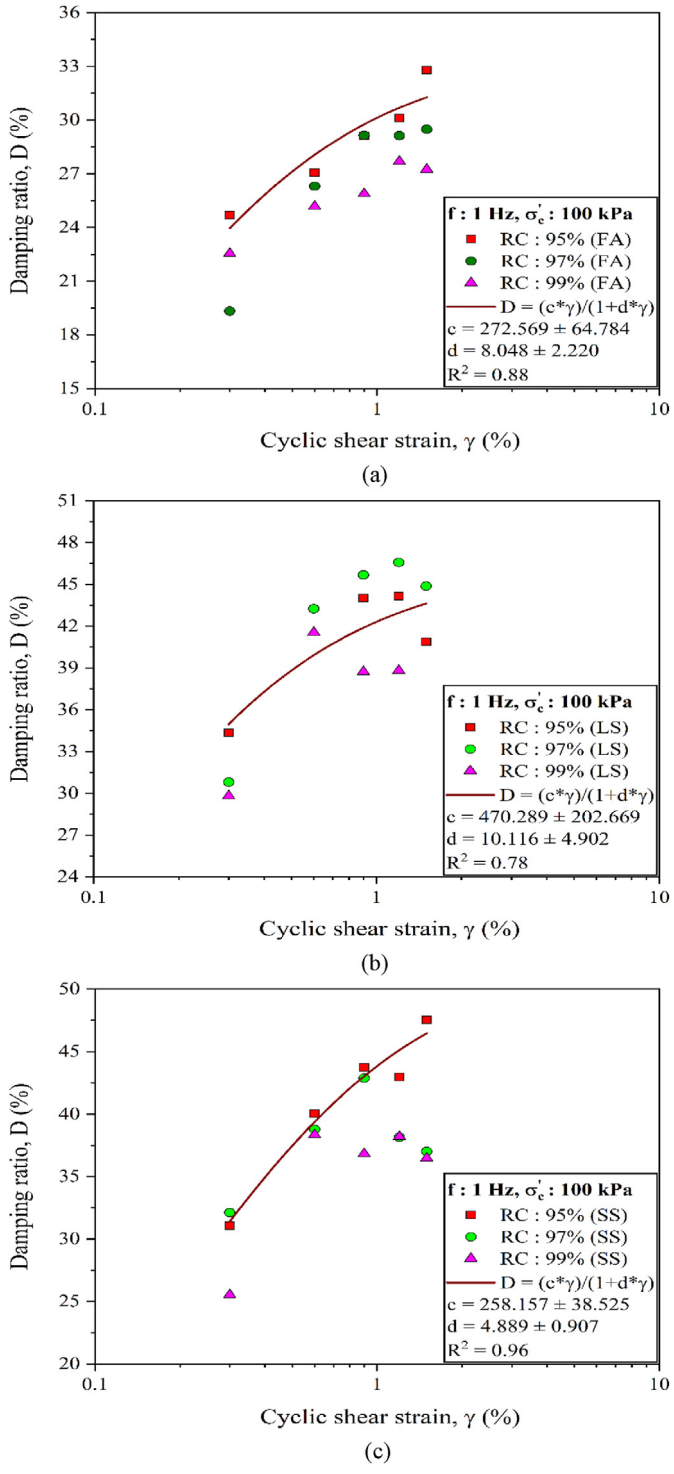

Fig. 16. Hyperbolic model fitting for damping ratio of fly ash, local soil, and stratified soil-ash samples test data.

14%, 5% and 8%, respectively. Similarly, in stratified soil-ash samples, these variations are 8%, 2% and 4% for the SHL, ASHL and ASTM approaches, respectively. However, local soil shows more or less the same damping estimated from the SHL approach for both the cycles and 5% & 2% variation for the ASHL and ASTM approaches. The relative compaction and confining pressure effects show similar variations in damping, but the change becomes more pronounced as the frequency of loading changes. Hence, from the above discussion, this can be concluded that the ASHL approach can be adapted to estimate the damping ratio using any cycle because this approach shows minimum variation than that of the others. Additionally, a critical strain must be identified because, below it, the cycle displays identical results, and beyond it, a substantial variation can be seen.

5.5. Comparison of present study results with past literature

The outcomes of the damping ratio of the present study under the influences of relative compaction (RC: 95%, 97%, 99%), confining pressure (CP: 70 kPa, 80 kPa, 100 kPa), and loading frequency (*f*: 0.3 Hz, 0.5 Hz, 1 Hz) are compared with the past reported results of soils (Figs. 13 and 14). Here, the damping ratio estimated from the ASHL (0th cycle) approach is used for comparison purposes. Because the ASHL approach is a novel approach that incorporates the unsymmetrical shape of the hysteresis loop for the precise estimation of the damping ratio. The soil types considered in the comparison are river sand, Toyoura sand, clay, sandy silt, gravelly rockfill, etc. (Kokusho, 1980; Vucetic and Dobry, 1991; Matasović and Vucetic, 1993; Kiku and Yoshida, 2000; Govindaraju, 2005; Ravishankar and Sitharam, 2005; Hanumantharao and Ramana, 2008; Araei et al., 2012; Kumar et al., 2014; Chiaradonna et al., 2015; Chattaraj and Sengupta, 2016; Amir-Faryar et al., 2017; Pagliaroli et al., 2018; Chehat et al., 2019; Li et al., 2020; Das and Chakrabortty, 2021; Mog and Anbazhagan, 2022). Additionally, the soil of various origins depicted in Fig. 15 is used to analyze the range of damping ratio of the current materials for a realistic interpretation. Kumar et al. (2017) investigated the damping behavior of Brahmaputra sand for large strain conditions using cyclic triaxial test and found that under large strain, the damping ratio increases till critical strain reaches its peak and then decreases. Since limited researchers had explored the dynamic behavior beyond 1%, thus it is recommended to perform dynamic testing further on this strain. So that critical strain can be identified for better seismic analysis of a particular soil. Specimen prepared at high density shows lower damping value compared to the samples prepared at low density and from Fig. 13a, this can be confirmed for the present materials. However, a contradictory result has been obtained by Mog and Anbazhagan (2022). Similarly, a specimen subjected to high confinement may impart high stiffness that in turn increases the shear modulus and decreases the damping ratio. The present results are in a good agreement with the past results illustrated in Fig. 13b. The high damping ratio obtained from the ASHL approach for the present materials is compared with the past results in Figs. 13 and 14. The SHL approach underestimates the damping value and the same can be seen in Figs. 8 and 9 and also similar trend has been observed by several researchers (Kumar et al., 2017; Das and Chakrabortty, 2021). The specimen subjected to a high loading frequency dissipates high energy which contributes to high damping values. From Fig. 14, this can be observed that irrespective of the material type, high frequency exhibits a high damping value. The damping value of the present fly ash is in a good agreement with the Sabarmati river sand and Xiamen standard sand (Ravishankar and Sitharam, 2005; Li et al., 2020). Mog and Anbazhagan (2022) performed a resonant column test on the sand and clayey samples and revealed that the clayey silt soils experience high damping value than that of the sandy soil. At large strain, each soil shows a damping value between 10% and 30% (Fig. 15), and the damping value estimated using the SHL approach is also coming within this range (Figs. 8 and 9). The trend of damping ratio with shear strain shows a good agreement with the past reported results. The damping assessment of any soil must be done for a wide strain (small-medium-large) range so that its complete profile can be established. Since this study was done only

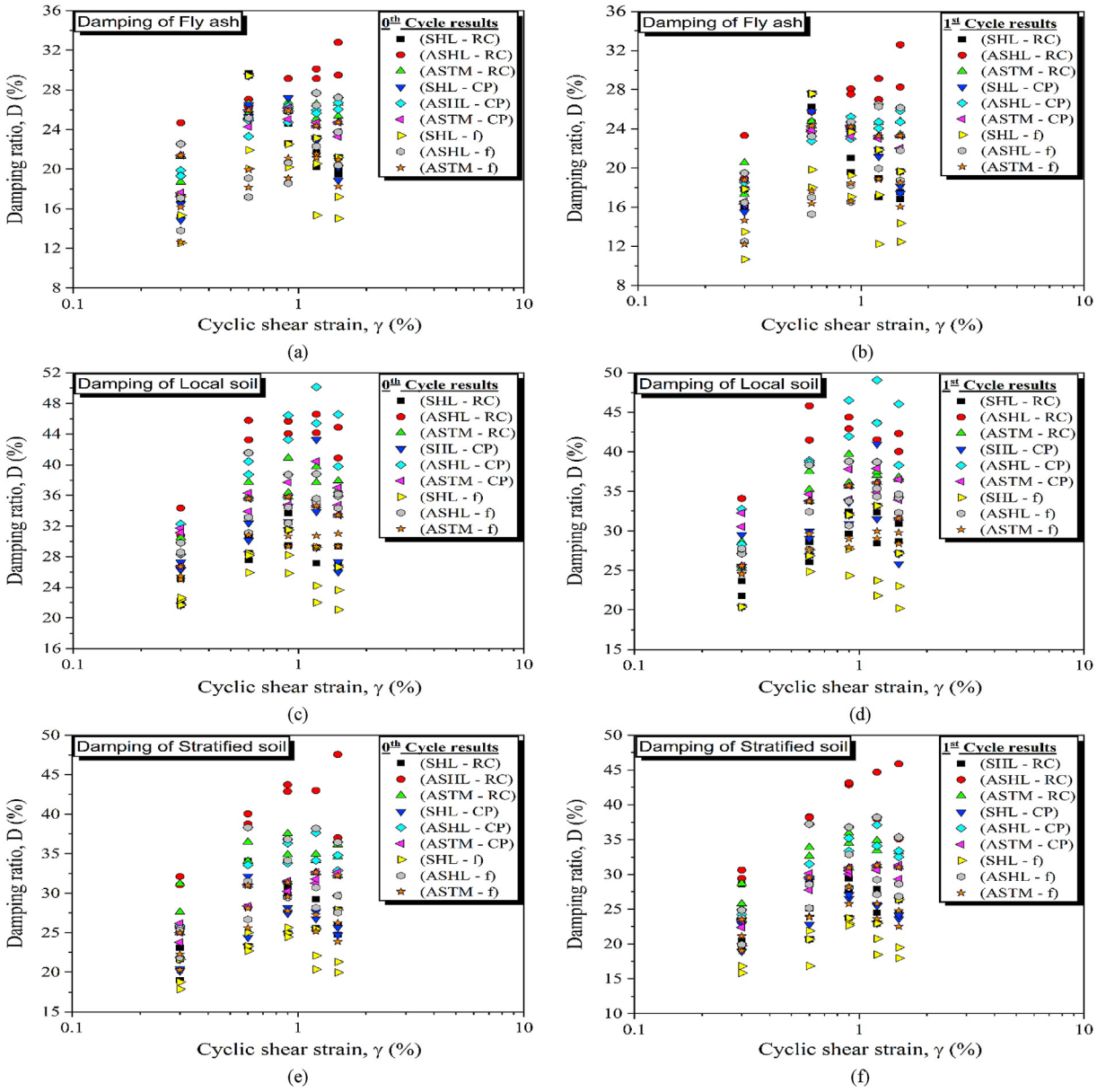

Fig. 17. Graphical representation of 0th and 1st cycle damping ratio for uniform and stratified soil-ash samples.

for large strain conditions that exhibit the limitation of the present study. A wide strain range can be considered the future scope of this research.

5.6. Model fitting of the present study results

Most of the researchers have given distinct damping estimation models for different types of soil such as clay, sand, gravelly soil and cohesionless soil (Hardin and Drnevich, 1972a, 1972b; Seed et al., 1986; Darendeli, 2001; Menq, 2003; Amir-Faryar, 2012). The limitation in the adaptability of the past fitting models is that it contains dissimilar dependent variables. Amir-Faryar et al. (2017) analyzed the existing empirical and other models available for the determination of the normalized shear modulus (G/G_{max}) and damping ratio (D) and reported a universal model for the G/G_{max} and D those are only dependent on the shear strain that can be applied to sand, clay, and fiber reinforced soil. A similar attempt has been taken by Wong et al. (2021) to provide an extended model for the cohesive soil that is dependent on the shear strain, effective stress, and plasticity index. The current experimental data were fitted in the universal model, however, only the uniform soil produced promising results, not the stratified soil. Hence, based on the availability of dependent parameters, the hyperbolic model has been adapted to fit the present experimental results. The fitting of the hyperbolic model for both the uniform and stratified soil-ash samples is shown in Fig. 16. It is found that the hyperbolic model shows a good agreement with the experimental results for the fly ash, local soil, and stratified soil-ash samples. Based on the results reported in Fig. 16, the hyperbolic model can be considered for the prediction of damping ratio in place of the universal model for present results, as the hyperbolic model contains two coefficients and shear strain as the dependent parameter. Apart from the model fitting, the variation of damping ratio estimated from the SHL, ASHL and ASTM methods for the 0th and 1st cycle positions is presented in Fig. 17 considering all the variables. From Fig. 17, it can be concluded that the stratified soil-ash and local soil illustrate the

higher variation in damping values followed by the fly ash. The soil has a higher damping ratio which expresses higher energy dissipation potential as in the case of stratified and local soils. Whereas fly ash has about 1.5 times low damping potential as compared with the other two. This also validates that irrespective of variable type, the damping ratio estimated from the ASHL method will always give higher results than that of the SHL method.

6. Conclusions

The damping behavior of fly ash, local soil, and their stratified system has been evaluated under large strain conditions using the cyclic triaxial test. The specimens were subjected to a large shear strain range of 0.3%–1.5% under the loading frequency of 0.3–1 Hz. In addition, the density of the compacted specimens was maintained between 95% and 99% of MDD and tested under a medium range of confining pressure (70–100 kPa). The present experimental study was carried out by applying high-strain amplitude loading that resulted in an unsymmetrical response of deviatoric stress versus axial strain. In order to analyze the unsymmetrical phenomena in the damping behavior of soil, the damping ratio was estimated by incorporating three different approaches such as SHL, ASHL and ASTM approaches. After examining the results reported above, several conclusions can be drawn that have been discussed below:

(1) The damping ratio of fly ash estimated from the symmetrical method (SHL) approach shows a similar trend, as in the case of the ASHL approach, and shows the maximum damping ratio at around 1% of shear strain.
(2) The specimens prepared under high density and subjected to high confinement show low damping ratios, whereas the specimens tested under high frequency show high damping behavior.
(3) The SHL approach is suitable for low-strain conditions because, under large-strain conditions, it underestimates the damping ratio of soils.
(4) Among all the approaches, the ASHL approach gives a higher damping ratio followed by the ASTM and then the SHL approach for fly ash, local soil, and stratified soil-ash samples.
(5) The influence of cycle position is not remarkable for low shear strain, but for the high strain, the difference in A_L is profound.
(6) The ASHL approach can be adopted for estimating the damping ratio using any cycle position data because this approach shows a minimum variation than that of the others.
(7) The maximum damping ratio of stratified deposit is always falling in between the damping ratio of local soil and fly ash. This is due to the combined interaction between fly ash and local soil.
(8) The peak of damping ratio of the fly ash varies between 0.6% and 0.9% of shear strain, however, the local soil shows a peak between 0.8% and 1.2% of shear strain. On the other hand, the stratified soil exhibits a wide range of damping ratio's peak variation, i.e. in the range of 0.6%–1% of shear strain.
(9) The stratified soil and local soil exhibit a slightly high damping ratio compared to different soils, whereas the damping ratio of fly ash is similar to the soil such as alluvium sand, Brahmaputra sand, and clayey soil.
(10) The hyperbolic model provides a good correlation for both the uniform and stratified soil-ash samples, whereas the universal model shows promising outcomes only for the uniform soil.

Declaration of competing interest

The authors declare that they have no known competing financial interests or personal relationships that could have appeared to influence the work reported in this paper.

Acknowledgments

The authors are grateful to the Department of Science and Technology, Government of India for providing financial assistance.

References

ACAA, 2003. Fly Ash Facts for Highway Engineers (FHWA-IF-03-019) (Aurora).
Amini, F., Chakravrty, A., 2004. Liquefaction testing of layered sand-gravel composites. Geotech. Test J. 27, 36–46.
Amini, F., Qi, G., 2000. Liquefaction testing of stratified silty sands. J. Geotech. Geoenviron. Eng. 126, 208–217.
Amini, F., Sama, K., 1999. Behaviour of stratified sand-silt-gravel composites under seismic liquefaction conditions. Soil Dynam. Earthq. Eng. 18, 445–455.
Amir-Faryar, B., 2012. Improvement of Dynamic Properties and Seismic Response of Clay Using Fiber Reinforcement. Doctoral dissertation, Department of Civil & Environmental Engineering, University of Maryland, College park, MD.
Amir-Faryar, B., Aggour, M.S., McCuen, R.H., 2017. Universal model forms for predicting the shear modulus and material damping of soils. Geomech. Geoeng. Int. J. 12, 60–71.
Araei, A.A., Razeghi, H.R., Ghalandarzadeh, A., Tabatabaei, S.H., 2012. Effects of loading rate and initial stress state on stress–strain behavior of rock fill materials under monotonic and cyclic loading conditions. Sci. Iran. 19, 1220–1235.
ASTM-D3999, 1996. Standard Test Methods for the Determination of the Modulus and Damping Properties of Soils Using the Cyclic Triaxial Apparatus (Philadelphia, United States).
ASTM-D698-12, 2012. Standard Test Methods for Laboratory Compaction Characteristics of Soil Using Standard Effort, 12 400 ft-lbf/ft3 (600 kN-m/m3 (Philadelphia, United States).
Ayoubi, P., Pak, A., 2017. Liquefaction-induced settlement of shallow foundations on two-layered subsoil strata. Soil Dynam. Earthq. Eng. 94, 35–46.
Bishop, A.W., Hight, D.W., 2015. The value of Poisson's ratio in saturated soils and rocks stressed under undrained conditions. Geotechnique 27, 369–384.
Borden, B.R.H., Shao, L., Gupta, A., 1996. Dynamic properties of piedmont residual soils. J. Geotech. Eng. 122, 813–821.
Bradshaw, A.S., Baxter, C.D.P., 2007. Sample preparation of silts for liquefaction testing. Geotech. Test J. 30, 324–332.
CAE., 2021. Report on Fly Ash Generation at Coal/Lignite Based Thermal Power Stations and its Utilization in the Country for the Year 2020 – 21 (New Delhi, India).
Chakrabortty, P., Roshan, A.R., Das, A., 2020. Evaluation of dynamic properties of partially saturated sands using cyclic triaxial tests. Indian Geotech. J. 50, 948–962.
Chandra, S., Kumari, R., Rajesh, S., 2016. Shear behavior of raebareli pond ash at low confining pressures. J. Solid Waste Technol. Manag. 42, 200–209.
Chattaraj, R., Sengupta, A., 2017. Dynamic properties of fly ash. J. Mater. Civ. Eng. 29, 1–9.
Chattaraj, R., Sengupta, A., 2016. Liquefaction potential and strain dependent dynamic properties of Kasai River sand. Soil Dynam. Earthq. Eng. 90, 467–475.
Chehat, A., Hussien, M.N., Abdellaziz, M., Chekired, M., Harichane, Z., Karray, M., 2019. Stiffness– and damping–strain curves of sensitive champlain clays through experimental and analytical approaches. Can. Geotech. J. 56, 364–377.
Chen, G.X., Liu, X.Z., Wang, B.H., 2007. Effect of variability of soil dynamic parameters on ground motion parameters for deep soft sites. J. Disaster Prev. Mitig. Eng. 27, 1–10.
Chiaradonna, A., Tropeano, G., D'Onofrio, A., Silvestri, F., Park, D., 2015. Application of a simplified model for the prediction of pore pressure build-up in sandy soils subjected to seismic loading. In: The 6th International Conference on Earthquake Geotechnical Engineering (Christchurch, New Zealand).
Dammala, P., Kumar, S., Krishna, A., Bhattacharya, S., 2019. Dynamic soil properties and liquefaction potential of northeast Indian soil for non-linear effective stress analysis. Bull. Earthq. Eng. 17, 2899–2933.
Dammala, P.K., Krishna, A.M., Bhattacharya, S., Nikitas, G., Rouholamin, M., 2017. Dynamic soil properties for seismic ground response studies in Northeastern India. Soil Dynam. Earthq. Eng. 100, 357–370.
Darendeli, M., 2001. Development of a New Family of Normalized Modulus Reduction and Material Damping Curves. Doctoral dissertation, University of Texas, Austin, TX.
Das, A., Chakrabortty, P., 2021. Large strain dynamic characteristics of quaternary alluvium sand with emphasis on empirical pore water pressure generation model. Eur. J. Environ. Civ. Eng. 1–24.
Dobry, R., Abdoun, T., 2015. Cyclic shear strain needed for liquefaction triggering and assessment of overburden pressure factor K σ. J. Geotech. Geoenviron. Eng. 141, 1–19.

Dutta, T.T., 2015. Dynamic Properties of Clean Sand and Expansive Clay from Resonant Column Studies. Doctoral dissertation, Department of Civil Engineering, Indian Institute of Technology - Hyderabad.
Fahoum, K., Aggour, M.S., Amini, F., 1996. Dynamic properties of cohesive soils treated with lime. J. Geotech. Eng. 122, 382–389.
Fiegel, G.L., Kutter, B.L., 1994. Liquefaction mechanism for layered soils. J. Geotech. Eng. 120, 737–755.
Figueroa, J.L., Saada, A.S., Liang, L., Dahisaria, N.M., 1994. Evaluation of soil liquefaction by energy principles. J. Geotech. Eng. 120, 1554–1569.
Govindaraju, L., 2005. Liquefaction and Dynamic Properties of Sandy Soils. Indian Institute of Science, Bangalore, India, 2005.
Govindaraju, L., Ramana, G., Hanumantharao, C., Sitharam, T., 2004. Site-specific ground response analysis. Curr. Sci. 87, 1354–1362.
Hanumantharao, C., Ramana, G., 2008. Dynamic soil properties for microzonation of Delhi, India. J. Earth Syst. Sci. 117, 719–730.
Hardin, B., Drnevich, V., 1972a. Shear modulus and damping in soils: design equations and curves. J. Soil Mech. Found. 98, 667–692.
Hardin, B.O., 1965. The nature of damping in sands. J. Soil Mech. Found Div. 91, 63–97.
Hardin, B.O., Drnevich, V.P., 1972b. Shear modulus and damping in soils: measurement and parameter effects. J. Soil Mech. Found Div. 98, 603–624.
Ingale, R., Patel, A., Mandal, A., 2017. Performance analysis of piezoceramic elements in soil: a review. Sens. Actuators Phys. 262, 46–63.
Ishihara, K., 1996. Soil Behaviour in Earthquake Geotechnics. Oxford University Press, Oxford, New York.
Ishihara, K., Troncoso, J., Kawase, Y., Takahashi, Y., 1980. Cyclic strength characteristics of tailings materials. Soils Found. 20, 127–142.
Jakka, R.S., Datta, M., Ramana, G.V., 2010. Liquefaction behaviour of loose and compacted pond ash. Soil Dynam. Earthq. Eng. 30, 580–590.
Jaya, V., Dodagoudar, G., Boominathan, A., 2012. Modulus reduction and damping curves for sand of south-east coast of India. J. Earthq. Tsunami 6, 1–19.
Jia, M., Wang, B., 2013. Liquefaction testing of stratified sands interlayered with silt. Appl. Mech. Mater. 256, 116–119.
Jin, J., Song, C., Liang, B., Chen, Y., Su, M., 2018. Dynamic characteristics of tailings reservoir under seismic load. Environ. Earth Sci. 77, 1–11.
Kalinski, M.E., Wallace, A.D., 2011. Laboratory measurement of the dynamic properties of fly ash. Geo-Frontiers - Adv. Geotech. Eng 1210–1216. American Society of Civil Engineers (ASCE).
Kiku, H., Yoshida, N., 2000. Dynamic deformation property tests at large strains. In: Proceeding of 12th World Conference on Earthquake Engineering (Auckland, New Zealand).
Kokusho, T., 2000. Correlation of pore-pressure B-value with P-wave velocity and Poisson's ratio for imperfectly saturated sand or gravel. Soils Found. 40, 95–102.
Kokusho, T., 1980. Cyclic triaxial test of dynamic soil properties for wide strain range. Soils Found. 20, 45–60.
Kokusho, T., Yoshida, Y., Esashi, Y., 1982. Dynamic properties of soft clay for wide strain range. Soils Found. 22, 1–18.
Konrad, J.M., Dubeau, S., 2003. Cyclic strength of stratified soil samples. In: Submarine Mass Movements and Their Consequences: 1st International Symposium. Springer, Dordrecht, Netherlands, pp. 47–57.
Kumar, J., 2012. Madhusudhan BN. Dynamic properties of sand from dry to fully saturated states. Geotechnique 62, 45–54.
Kumar, S.S., Dey, A., 2015. 1D ground response analysis to identify liquefiable substrata: case study from Guwahati city. In: Ukieri Workshop on Seismic Requalification of Pile Supported Structures. SRPSS) Guwahati, India.
Kumar, S.S., Dey, A., Krishna, A.M., 2014. Equivalent linear and nonlinear ground response analysis of two typical sites at Guwahati city. In: Proceeding of Indian Geotechnical Conference (Kakinada, India).
Kumar, S.S., Krishna, A.M., Dey, A., 2018. Dynamic properties and liquefaction behaviour of cohesive soil in northeast India under staged cyclic loading. J. Rock Mech. Geotech. Eng. 10, 958–967.
Kumar, S.S., Krishna, A.M., Dey, A., 2017. Evaluation of dynamic properties of sandy soil at high cyclic strains. Soil Dynam. Earthq. Eng. 99, 157–167.
Ladd, R.S., 1978. Preparing test specimens using undercompaction. Geotech. Test J. 1, 16–23.
Li, J., Cui, J., Shan, Y., Li, Y., Ju, B., 2020. Dynamic shear modulus and damping ratio of sand–rubber mixtures under large strain range. Mater 13, 1–29.
Liao, H.J., Cheng, S.H., Quo, L.W., Wong, R.K., Chien, P.Y., 2012. Properties of hydraulically dumped coal ash after soil mixing improvement. In: The Proceedings of the Fourth International Conference on Grouting Deep Mixing, pp. 1373–1384, 2012.
Mashiri, M.S., 2014. Monotonic and cyclic behaviour of sand-tyre chip (STCh) mixtures. In: Doctoral Dissertation, School of Civil, Mining and Environmental Engineering. University of Wollongong.
Matasović, N., Vucetic, M., 1993. Cyclic characterization of liquefiable sands. J. Geotech. Eng. 119, 1805–1822.
Menq, F., 2003. Dynamic Properties of Sandy and Gravelly Soils. Doctoral Dissertation, University of Texas, Austin.
Ministry of Coal, 2020. Year End Review 2020. Ministry of Coal, Delhi, India.
Mog, K., Anbazhagan, P., 2022. Evaluation of the damping ratio of soils in a resonant column using different methods. Soils Found. 62, 1–21.
Mohanty, S., Patra, N.R., 2016. Dynamic response analysis of Talcher pond ash embankment in India. Soil Dynam. Earthq. Eng. 84, 238–250.
Mulilis, J.P., Chan, C.K., Seed, H.B., 1975. The effects of method of sample preparation on the cyclic stress-strain behavior of sands. In: Report No. UCB/EERC-75/18 (Berkeley, California).
Mulilis, J.P., Seed, H.B., Chan, C.K., Mitchell, J.K., Arulanandan, K., 1977. Effects of sample preparation on sand liquefaction. J. Geotech. Eng. Div. 103, 91–108.
Naresh, D., 2010. Management of ash disposal. In: The Proceeding of Indian Geotechnical Conference Bombay, pp. 113–120. India.
Nogami, Y., Murono, Y., Morikawa, H., 2012. Nonlinear hysteresis model taking into account S-shaped hysteresis loop and its standard parameters. In: The Proceeding of The15th World Conference on Earthquake Engineering. Portugalia, Lisboa.
Pagliaroli, A., Aprile, V., Chamlagain, D., Lanzo, G., Poovarodom, N., 2018. Assessment of site effects in the Kathmandu Valley, Nepal, during the 2015 Mw 7.8 Gorkha earthquake sequence using 1D and 2D numerical modelling. Eng. Geol. 239, 50–62.
Paul, S., Dey, A., 2007. Cyclic triaxial testing of fully and partially saturated soil at silchar. In: The Proceeding of the 4th International Conference on Earthquake Geotechnical Engineering, pp. 1–12. Thessaloniki, Greece.
Puri, N., Jain, A., Nikitas, G., Dammala, P.K., Bhattacharya, S., 2020. Dynamic soil properties and seismic ground response analysis for North Indian seismic belt subjected to the great Himalayan earthquakes. Nat. Hazards 103, 447–478.
Ram, A.K., Mohanty, S., 2021. Experimental investigation on dynamic behavior of silt-rich fly ash using cyclic triaxial and bender element tests. Innov. Infrastruct. Solut. 6, 1–24.
Ravishankar, B., Sitharam, T., 2005. Govindaraju L. Dynamic properties of Ahmedabad sands at large strains. In: The Proceeding of Indian Geotechnical Conference, pp. 369–372. Ahmedabad, India.
Reddy, M.V.R.K., Mohanty, S., Rehana, S., 2020. Experimental investigation on dynamic characterization of equi-proportionate silt–sand range pond ash at high strain. Int. J. Geosynth. Gr. Eng. 6, 1–14.
Santos, J.A., Correia, A.G., 2000. Shear Modulus of soils under cyclic loading at small and medium strain level. In: The Proceeding of 12th World Conference on Earthquake Engineering (Auckland, New Zealand).
Saride, S., Dutta, T.T., 2016. Effect of fly-ash stabilization on stiffness modulus degradation of expansive clays. J. Mater. Civ. Eng. 28, 04016166.
Seed, H.B., Wong, R.T., Idriss, I.M., Tokimatsu, K., 1986. Moduli and damping factors for dynamic analyses of cohesionless soils. J. Soil Mech. Found Div. 112, 1016–1032.
Shah, D., Narayan, S., 2020. Coal Ash in India: A Compendium of Disasters. environmental and health risks, Chennai, India.
Shinde, N.S., Kumar, J., 2022. Assessing the liquefaction potential of a sand specimen by using resonant column test. Soil Dynam. Earthq. Eng. 159, 1–15.
Singh, H.P., Maheshwari, B.K., Saran, S., Paul, D.K., 2008. Evaluation of liquefaction potential of pond ash. In: Geotechnical Engineering for Disaster Mitigation and Rehabilitation: Proceedings of the 2nd International Conference GEDMAR08 (Nanjing, China).
Sitharam, T.G., Anbazhagan, P., 2008. Seismic microzonation: principles, practices and experiments. Electron. J. Geotech. Eng. 8, 1–58.
Sitharam, T.G., Vinod, J.S., Ravishankar, B.V., 2009. Post-liquefaction undrained monotonic behaviour of sands: experiments and DEM simulations. Geotechnique 59, 739–749.
Tipraj, B., Prasad, M.G., Prasanna, E.L., Priyanka, A., Hugar, P., 2019. Strength characteristics of concrete with partial replacement of cement by fly ash and activated fly ash. Int. J. Recent Technol. Eng. 34, 1–7.
Tsuchida, H., 1970. Prediction and counter measure against the liquefaction in sand deposits. In: The Abstract of the Seminar in the Port and Harbor. Research Institute, pp. 31–333.
Tsukamoto, Y., Ishihara, K., Sawada, S., 2004. Settlement of silty sand deposits following liquefaction during earthquakes. Soils Found. 44, 135–148.
Vaid, Y., Negussey, D., 1988. Preparation of Reconstituted Sand Specimens. Advanced Triaxial Testing of Soil and Rock, 977. ASTM STP, pp. 405–417.
Vasquez-Herrera, A., Dobry, R., 1989. Re-evaluation of the lower san fernando dam. In: Report 3. The Behavior of Undrained Contractive Sand and its Effect on Seismic Liquefaction Flow Failures of Earth Structures. Army Engineer Waterways Experiment Station Vicksburg MS Geotechnical Lab, Washington, DC.
Vucetic, M., Dobry, R., 1991. Effect of soil plasticity on cyclic response. J. Geotech. Eng. 117, 89–107.
Vucetic, M., Dobry, R., 1988. Cyclic triaxial strain-controlled testing of liquefiable sands. Advanced triaxial testing of soil and rock. ASTM STP 977, 475–488.
Wong, J.K.H., Wong, S.Y., Wong, K.Y., 2021. Extended model of shear modulus reduction for cohesive soils. Acta Geotech 21, 1–17.
Xiu, Z., Wang, S., Ji, Y., Wang, F., Ren, F., 2020. Experimental investigation on liquefaction on liquefaction and post-liquefaction deformation of stratified saturated sand under cyclic loading. Bull. Eng. Geol. Environ. 79, 2313–2324.
Yokota, K., Konno, M., 1980. Dynamic Poisson's ratio of soil. In: The Proceedings of the 7th World Conference on Earthquake Engineering Istanbul (Turkey).
Yoshimine, M., Koike, R., 2005. Liquefaction of clean sand with stratified structure due to segregation of particle size. Soils Found. 45, 89–98.
Yoshimoto, N., Orense, R.P., Hyodo, M., Nakata, Y., 2014. Dynamic behavior of granulated coal ash during earthquakes. J. Geotech. Geoenviron. Eng. 140, 1–11.
Zhang, J., Andrus, R.D., Juang, C.H., 2005. Normalized shear modulus and material damping ratio relationships. J. Geotech. Geoenviron. Eng. 131, 453–464.

Amit Kumar Ram obtained his Bachelor's degree in Civil Engineering from Faculty of Engineering and Technology, Agra, India, in 2015, and his Master's degree in Geotechnical Engineering from Indian Institute of Technology (Banaras Hindu University), Varanasi, India. Currently, he is a research scholar in the Geotechnical Engineering Division at Indian Institute of Technology (Banaras Hindu University), Varanasi, India. He is working in the areas of waste utilization, dynamic characterization, geotechnical earthquake engineering, pavement geotechnics, liquefaction susceptibility, and dynamic response analysis.

Dr. Supriya Mohanty is working as an Assistant Professor in the Department of Civil Engineering at Indian Institute of Technology (BHU), Varanasi, India. She received her PhD in Civil Engineering from Indian Institute of Technology Kanpur, India, and her BTech degree in Civil Engineering from Veer Surendra Sai University of Technology, Burla, Odisha, India. Her research interests are liquefaction potential evaluation, soil dynamics and geotechnical earthquake engineering.